ISSN 2523-6784

Volume 6, Issue 18 – January – June - 2022

Journal of Systematic Innovation

ECORFAN®

Journal of Systematic Innovation, Volume 6, Issue 18, January - June 2022, is a journal edited six monthly by ECORFAN-Taiwan. Taiwan, Taipei. YongHe district, ZhongXin, Street 69. Postcode: 23445. WEB: www.ecorfan.org/taiwan, revista@ecorfan.org. Chief Editor: IGLESIAS-SUAREZ, Fernando. MsC. ISSN-On line: 2523-6784. Responsible for the latest update of this number ECORFAN Computer Unit. ESCAMILLA-BOUCHÁN, Imelda, PhD, LUNA-SOTO, Vladimir. PhD. Taiwan, Taipei. YongHe district, ZhongXin, Street 69, last updated June 30, 2022.

Journal of Systematic Innovation

Definition of Journal

Scientific Objectives

Support the international scientific community in its written production Science, Technology and Innovation in the Field of Engineering and Technology, in Subdisciplines of electromagnetism, electrical distribution, sources innovation in electrical, engineering signal, amplification electrical, motor design science, materials in electrical power, plants management and distribution of electrical energies.

ECORFAN-Mexico SC is a Scientific and Technological Company in contribution to the Human Resource training focused on the continuity in the critical analysis of International Research and is attached to CONACYT-RENIECYT number 1702902, its commitment is to disseminate research and contributions of the International Scientific Community, academic institutions, agencies and entities of the public and private sectors and contribute to the linking of researchers who carry out scientific activities, technological developments and training of specialized human resources with governments, companies and social organizations.

Encourage the interlocution of the International Scientific Community with other Study Centers in Mexico and abroad and promote a wide incorporation of academics, specialists and researchers to the publication in Science Structures of Autonomous Universities - State Public Universities - Federal IES - Polytechnic Universities - Technological Universities - Federal Technological Institutes - Normal Schools - Decentralized Technological Institutes - Intercultural Universities - S & T Councils - CONACYT Research Centers.

Scope, Coverage and Audience

Journal of Systematic Innovation is a Journal edited by ECORFAN-Mexico S.C in its Holding with repository in Taiwan, is a scientific publication arbitrated and indexed with semester periods. It supports a wide range of contents that are evaluated by academic peers by the Double-Blind method, around subjects related to the theory and practice of electromagnetism, electrical distribution, sources innovation in electrical, engineering signal, amplification electrical, motor design science, materials in electrical power, plants management and distribution of electrical energies with diverse approaches and perspectives, that contribute to the diffusion of the development of Science Technology and Innovation that allow the arguments related to the decision making and influence in the formulation of international policies in the Field of Engineering and Technology. The editorial horizon of ECORFAN-Mexico® extends beyond the academy and integrates other segments of research and analysis outside the scope, as long as they meet the requirements of rigorous argumentative and scientific, as well as addressing issues of general and current interest of the International Scientific Society.

Editorial Board

Arbitration Committee

Assignment of Rights

The sending of an Article to Journal of Systematic Innovation emanates the commitment of the author not to submit it simultaneously to the consideration of other series publications for it must complement the Originality Format for its Article.

The authors sign the Authorization Format for their Article to be disseminated by means that ECORFAN-Mexico, S.C. In its Holding Taiwan considers pertinent for disclosure and diffusion of its Article its Rights of Work.

Declaration of Authorship

Indicate the Name of Author and Coauthors at most in the participation of the Article and indicate in extensive the Institutional Affiliation indicating the Department.

Identify the Name of Author and Coauthors at most with the CVU Scholarship Number-PNPC or SNI-CONACYT- Indicating the Researcher Level and their Google Scholar Profile to verify their Citation Level and H index.

Identify the Name of Author and Coauthors at most in the Science and Technology Profiles widely accepted by the International Scientific Community ORC ID - Researcher ID Thomson - arXiv Author ID - PubMed Author ID - Open ID respectively.

Indicate the contact for correspondence to the Author (Mail and Telephone) and indicate the Researcher who contributes as the first Author of the Article.

Plagiarism Detection

All Articles will be tested by plagiarism software PLAGSCAN if a plagiarism level is detected Positive will not be sent to arbitration and will be rescinded of the reception of the Article notifying the Authors responsible, claiming that academic plagiarism is criminalized in the Penal Code.

Arbitration Process

All Articles will be evaluated by academic peers by the Double Blind method, the Arbitration Approval is a requirement for the Editorial Board to make a final decision that will be final in all cases. MARVID® is a derivative brand of ECORFAN® specialized in providing the expert evaluators all of them with Doctorate degree and distinction of International Researchers in the respective Councils of Science and Technology the counterpart of CONACYT for the chapters of America-Europe-Asia- Africa and Oceania. The identification of the authorship should only appear on a first removable page, in order to ensure that the Arbitration process is anonymous and covers the following stages: Identification of the Journal with its author occupation rate - Identification of Authors and Coauthors - Detection of plagiarism PLAGSCAN - Review of Formats of Authorization and Originality-Allocation to the Editorial Board-Allocation of the pair of Expert Arbitrators-Notification of Arbitration -Declaration of observations to the Author-Verification of Article Modified for Editing-Publication.

Instructions for Scientific, Technological and Innovation Publication

Knowledge Area

The works must be unpublished and refer to topics of electromagnetism, electrical distribution, sources innovation in electrical, engineering signal, amplification electrical, motor design science, materials in electrical power, plants management and distribution of electrical energies and other topics related to Engineering and Technology.

Presentation of the content

In the first article we present, *Implementation of a system for classifying moving parts by color* by RODRÍGUEZ-FRANCO, Martín Eduardo, LÓPEZ-ÁLVAREZ, Yadira Fabiola, JARA-RUIZ, Ricardo and OROZCO-SOTO, Santos Miguel, with adscription in the Universidad Tecnológica del Norte de Aguascalientes and University of Naples Federico II, in the next article we present, *Mathematical analysis for the selection of the heating equipment of the hot forming stamping* by HUERTA-GÁMEZ, Héctor, CERRITO-TOVAR, Iván de Jesús, PÉREZ-PÉREZ, Arnulfo and TORRES-MENDOZA, Raymundo Esteban, with adscription in the Universidad Politécnica Juventino Rosas, in the next article we present, *Analysis and dynamic simulation of the cardan shaft for the minilow prototype vehicle* by AGUILAR-MORENO, Antonio Alberto, GARCIA-DUARTE, Oscar Enrique, ARELLANO-PATIÑO José Antonio and ALVAREZ-GARCIA, Eduardo, with adscription in the Universidad Politécnica de Juventino Rosas, in the last article we present, *Adjustable testbench system to stretch optical fiber* by TALAVERA-VELÁZQUEZ Dimas, MARTÍNEZ-TELLO Josué, GUTIÉRREZ-VILLALOBOS José Marcelino and RIVAS-ARAIZA Edgar Alejandro, with adscription in the Universidad de Guanajuato Campus Celaya-Salvatierra and Universidad Autónoma de Querétaro.

Content

Article **Journal of Systematic Innovation**
June 2022 Vol.6 No.18 1-10

Implementation of a system for classifying moving parts by color

Implementación de sistema para la clasificación de piezas en movimiento por color

RODRÍGUEZ-FRANCO, Martín Eduardo†*[1], LÓPEZ-ÁLVAREZ, Yadira Fabiola[1], JARA-RUIZ, Ricardo[1] and OROZCO-SOTO, Santos Miguel[2]

[1]*Universidad Tecnológica del Norte de Aguascalientes, Rincón de Romos, Aguascalientes, México*
[2]*University of Naples Federico II, Naples, Campania, Italy*

ID 1st Author: *Martín Eduardo, Rodríguez-Franco* / **ORC ID**: 0000-0002-6804-4777, **Researcher ID Thomson**: T-1539-2018, **CVU CONACYT ID**: 660892.

ID 1st Co-author: *Yadira Fabiola, López-Álvarez* / **ORC ID**: 0000-0002-9041-1908, **Researcher ID Thomson**: T-1555-2018, **CVU CONACYT ID**: 375952

ID 2nd Co-author: *Ricardo, Jara-Ruiz* / **ORC ID**: 0000-0001-7725-4138, **Researcher ID Thomson**: T-1532-2018, **CVU CONACYT ID**: 630276

ID 3rd Co-author: *Santos Miguel, Orozco-Soto* / **ORC ID**: 0000-0001-6191-4306

DOI: 10.35429/JSI.2022.18.6.1.10 Received March 14, 2021; Accepted June 29, 2021

Abstract

The purpose of this study is the development and implementation of a computer vision system for color identification in a set of parts, which were disposed on a continuously moving conveyor belt. The process for acquiring the images associated with the parts at issue, the preprocessing and treatment phases performed, as well as the results of the recognition of the feature of interest in each of these are exposed. It is worthy to mention that the feature of interest in the analyzed parts was established from three classes different, associated with the primary colors. The results obtained suggest the effectiveness of the implemented vision system, even as a prototype; which was integrated using low-cost and easy-to-use materials, and whose programming was developed in the open-source software Python, using the OpenCV library. Not only an effective recognition of the class corresponding to each part entered is highlighted, but also the possibility that said operation be executed without the conveyor belt used stopping its moving.

Computer vision, Color identification, Moving parts tracking

Resumen

El presente estudio tiene por propósito el desarrollo e implementación de un sistema de visión por computadora para la identificación del color en un conjunto de piezas, las cuales fueron dispuestas sobre una banda transportadora en movimiento continuo. Se expone el proceso para la adquisición de las imágenes asociadas a las piezas en cuestión, las fases del preprocesamiento y tratamiento ejecutados, así como los resultados del reconocimiento de la característica de interés en cada una de éstas; misma que fue establecida a partir de tres clases distintas, asociadas a los colores primarios. Los resultados obtenidos sugieren la efectividad en el funcionamiento del sistema de visión implementado, aun como un prototipo; el cual fue integrado empleando materiales de bajo costo y fácil manejo, y cuya programación fue desarrollada en software de código abierto: Python, y la librería OpenCV. Se resalta, no únicamente un reconocimiento efectivo de la clase correspondiente a cada pieza ingresada, sino la posibilidad de que dicha operación sea ejecutada sin que la banda transportadora utilizada detuviera su recorrido.

Visión por computadora, Identificación de color, Seguimiento de piezas en movimiento

Citation: RODRÍGUEZ-FRANCO, Martín Eduardo, LÓPEZ-ÁLVAREZ, Yadira Fabiola, JARA-RUIZ, Ricardo and OROZCO-SOTO, Santos Miguel. Implementation of a system for classifying moving parts by color. Journal of Systematic Innovation. 2022. 6-18: 1-10

* Correspondence to Author (e-mail: martin.rodriguez@utna.edu.mx)
† Researcher contributing as first author.

Introduction

In recent decades, the evolution of inspection systems has left aside manual tasks, performed by people, to focus on the use of the computer as a means for the automatic execution of such a function (Xiao-bo, Jie-wen, Yanxiao, & Holmes, 2010) (Patel, Kar, Jha, & Khan, 2012). From this fact, various industrial activities have benefited, including the selection of fruits and vegetables (Vijayarekha, 2012) (Zhang, y otros, 2014), food safety assurance (Dowlati, de la Guardia, & Mohtasebi, 2012) (Jackman & Sun, 2013) and, the manufacturing and assembly of mechanical elements (Barari, 2013) (Ayub, Mohamed, & Esa, 2014), among others. Thus, automatic inspection systems are developed from the application of artificial vision techniques, which encompasses the study of methods for understanding and encrypting an analyzed image, from a computer, in order to obtain certain characteristics. that are of interest (Santos-Gomes & Rodrigues-Leta, 2012). In this way, a computer vision system can be considered as an integration of mechanical elements, sensors and instrumentation, digital video systems and image processing techniques (Patel, Kar, Jha, & Khan, 2012).

On the other hand, image preprocessing includes the use of operations to improve its quality, through noise reduction, contrast improvement and the definition of captured shapes (Kodagali & Balaji, 2012). After preprocessing, the segmentation, description and recognition of individual objects present in the captured image are necessary, from the extraction of study attributes, such as edges, contours, areas, etc. Finally, the application of cognitive functions, associated with vision, is required to provide a sense to the recognized object as a whole (Xiao-bo, Jie-wen, Yanxiao, & Holmes, 2010).

It is worth mentioning that, at present, various industrial operations perform automated inspection tasks of processed parts on a moving conveyor belt. Such an attachment is one of the main components of a typical material handling system (Bozma & Yalçın, 2002), on which objects are briefly positioned to be transported between two different points of a production process (Selver, Akay, Alim, Bardakçı, & Ölmez, 2011). By means of a camera, usually placed above the conveyor, that each object that moves along it is visualized (Tran, 2019).

Motivation

Given the relevance of computer vision systems in the current industrial environment, and particularly, of its application as a central element in automated inspection, it is of great interest in the technological academic field, the study of the elements that comprise it, as well as the role they perform together. Such is the importance conferred to these systems, which are part of the subject topics for various Engineering profiles; therefore, an exploration in great detail of their capabilities can bring with it knowledge of their functionality, prior to having contact with them in the industry.

However, since having a vision system with the features of those used in large transformation companies, means a heavy expense, it is possible to resort to the creation of a prototype, made up of elements that are easy to use, low cost and with acceptable performance. Likewise, based on the evolution of computing and the proposal of increasingly competitive programming languages and specialized libraries, it is possible to develop sophisticated artificial vision algorithms, without resorting to complex equipment or high processing demand, but that they can be executed from a personal computer.

Additionally, the process of designing the functionality of a vision system for automated inspection purposes implies understanding its structuring phases, starting from its base elements: software and hardware. Therefore, the need and challenge of conforming both the physical portion, as means for image acquisition, and developing its virtual counterpart, to ensure the processing of these and the extraction of the useful characteristics for the analysis undertaken, is assumed. In this way, the proposed process can encompass a set of tasks that enrich the experience of the participants.

Conveyor belt prototype

The conveyor belt used, shown in figure 1, was created from two side walls manufactured in rectangular hollow sections (RHS); at whose ends are located the supports that give them height.

ISSN 2523-6784

The separation between walls was established by metal rollers screwed to them; one of which allows the tension adjustment of the belt itself. The belt used is made of black rubber, whose ends were joined to form a closed loop. Likewise, a direct current electric motor with mechanical reducer is used, powered at 12 V; which is attached to one of the end rollers of the band to induce movement, at a rate of 0.157 ft./s (0.048 m/s).

Figure 1 Conveyor belt used
Source: Own Elaboration, 2022

An inspection area has been adapted to the conveyor described, consisting of two walls and a flap, made of sheets of steel sheet, and joined together. The walls were welded to those of the band, from four steel angle bars, which also support the upper portion. On the latter, a base was adapted for the location of the camera, being manufactured in polylactic acid (PLA) by 3D printing. Curtains were placed on the open ends, whose function is to allow parts access to the inspection area, while it remains isolated from external lighting.

Structure and function of vision systems

A computer vision system is mainly made up of five basic elements: lighting, camera, image capture card, software and hardware, as shown in figure 2. Other complementary elements to the vision system can be image filters and the guided means for the transportation of the digitized image and the communication between devices (Dowlati, de la Guardia, & Mohtasebi, 2012) (Zhang, y otros, 2014).

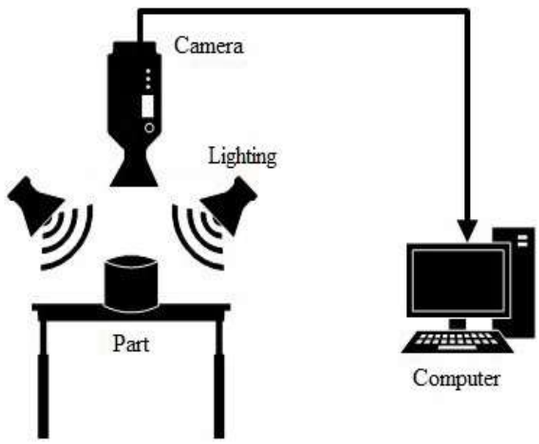

Figure 2 Computer vision system structure
Source: Own Elaboration, 2022

The camera is the main component of the vision system, performing image acquisition. The captured image is a matrix of tiny photosensitive elements; whose shutter is proportional to the amount of incident light. An image capture card is used to identify the frame of an object, and then store it in a compressed form (Wu & Sun, 2013). Meanwhile, the hardware and software work together for the analysis of the acquired image, the extraction of the features of interest and the execution of the classification task. Such actions are similar to those performed by the human brain (Ayub, Mohamed, & Esa, 2014) (Wang, Wang, Chen, & Xu, 2018).

Similar to human eyes, computer vision systems are affected by the level and quality of lighting. Such property is applied to the objects to be inspected, therefore, the control in the intensity and effectiveness of the lighting system used, determines, in turn, the effectiveness in the processing of the acquired images (Wang, Wang, Chen, & Xu, 2018), by reducing disturbances inherent to this process (Kodagali & Balaji, 2012).

The main interest of the processing and analysis of the images, obtained from the application of a computer vision system, is to constitute an informative, significant and explicit description of the physical object of interest (Brosnan & Sun, 2004) (Dowlati, de la Guardia, & Mohtasebi, 2012). For which, algorithms will have to be developed and applied that allow the subsequent execution of object classification or measurement tasks (Ye, Dong, & Liu, 2016), through the fulfillment of the following stages:

ISSN 2523-6784

1. Acquisition of images and their conversion to a digital format.

2. Improvement of the characteristics of the image for its pre-processing.

3. Segmentation of the digital image to separate non-overlapping regions.

4. Obtaining the characteristics of the object of interest in the image.

5. Classification for the identification of the object through groups of classes.

Operation of the proposed system

The proposed computer vision system will have to identify the color and area attributes of the parts that are placed on a first end of the used conveyor belt. Each part deposited on the belt will be taken inside the inspection area, and when detected by the camera, a contour will be drawn on its edge, of the respective color.

This contour represents the result of the visual classification executed on each part entered, based on the feature of color; being established three categories: red, green and blue. It should be noted that the conveyor will never stop moving.

Thus, when executing the capture of images corresponding to the parts on the moving belt, the camera will play a vital role for the implemented vision system. In this case, it is a Genius FaceCam 321 model camera, shown in figure 3, whose specifications are presented in table 1.

The focus of such camera has been oriented inside the confined space by the inspection cabin, adapted above the belt. The focal point of the camera was placed at a horizontal distance of 4.331 in (11 cm) and a vertical distance of 4.134 in (10.5 cm), both with respect to the lower left corner that forms the roof of the cabin used.

Figure 3 Genius FaceCam 321 camera
Source: https://us.geniusnet.com, 2022

Feature	Specification
Weight	1.764 oz (50 g)
Height	2.362 in (6 cm)
Width	1.772 in (4.5 cm)
Depth	1.575 in (4 cm)
Software	Arcsoft WCC4 Lite Arcsoft MiVE Genius Utility
Minimum processor	Intel/AMD 1.6 GHz
Minimum RAM	512 MB
Interface	USB 2.0
Sensor type	CMOS
Mounting type	Clip/Stand
Digital zoom	3X
Resolution	8 Mpx
Video formats supported	M-JPEG, WMV
Maximum video resolution	640 x 480 px
Maximum frame rate	30 pps

Table 1 Technical details of Genius FaceCam 321 camera
Source: https://us.geniusnet.com, 2022

As the camera was placed above the inspection compartment, in addition to being viewed at a vertical distance of 0.886 ft. (27 cm) above the conveyor belt, it was possible to establish a 0.656 x 0.525 ft. (20 x 16 cm) surface captured by the shot. Therefore, it should be noted that the aforementioned area exclusively ensures the visualization of the portion of the belt and, once the corresponding tests have been performed, the appreciation of each of the objects that move through it. Such a ratio was determined by the focal length between the camera lens and its field of view.

Likewise, in order to preserve the adequate lighting conditions for color recognition in the parts to be processed, cold white light-emitting diodes (LEDs) were adapted inside the inspection space.

ISSN 2523-6784

These devices were located in proximity to the upper corners inside the cabin, so that their orientation allows the lighting to be assigned and uniformly affect the upper face of each part entered. This decision was made given that, since the upper face of the parts is fully captured by the camera, this will be the reference for the subsequent processing that will be executed on the acquired image.

Algorithm for part classification

The preparation of the inspection cabin, the establishment of the camera capture area, and the calibration of the lighting system used, allowed to continue with the development of the visual classification algorithm of parts, as well as the performance of the initial tests on them in order to validate its effectiveness. It will be common that in the image analysis and processing sections, the term "object" be used to refer to the area of interest detected and that stands out from the background in a specific image; unlike "part", which will refer to the physical element of interest, in which the features from which this analysis is applied converge.

The algorithm used for the classification of parts was programmed in the Python Integrated Development and Learning Environment (IDLE), through functions from the OpenCV library, whose purpose is the acquisition and processing of images and video. The flow in the developed programming includes the stages shown in figure 4.

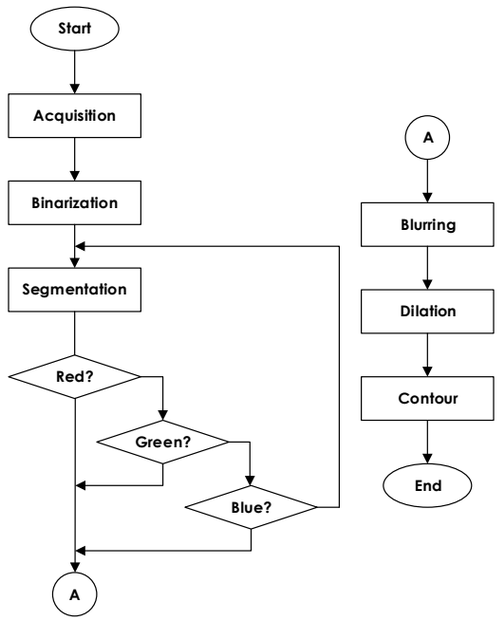

Figure 4 Algorithm for part classification by color
Source: Own Elaboration, 2022

Image acquisition

Image acquisition is determined by light reflected, transmitted or emitted from the beam arrangement received by the camera and radiation from the illumination system, which can illuminate, transmit through, reflect or absorb after interacting with the object studied (Zhang, y otros, 2014). Therefore, having a space that is properly isolated from the outside and uniformly lit is critical for this process. It is worth mentioning that the surface defined for the camera focus, and that frames the width of the belt, ensures the capture of any point on it; where a particular disposition of each part to be analyzed is not required; as highlighted in figure 5. It is even possible that the analyzed part adopts any orientation on the belt, without this affecting the effectiveness of subsequent processing.

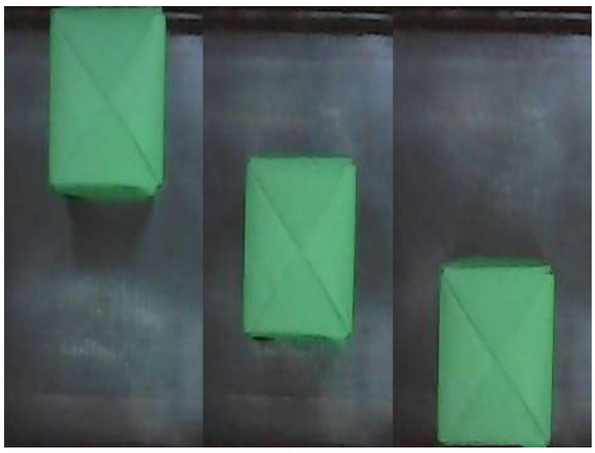

a) b) c)

Figure 5 Part capture on the belt at: a) upper end, b) center and c) lower end
Source: Own Elaboration, 2022

Image binarization

The preprocessing of each acquired image begins with the binarization or thresholding operation, which distinguishes only two classes in a captured image: the object of interest and the background that contains it. This process is based on the imposition of a threshold intensity value, from which the portions of the image with an intensity equal to or greater will be represented completely white, while those below will appear black. Such an operation confers the features of computational simplicity, high speed and zero complications in its implementation (Tavakoli & Najafzadeh, 2015).

ISSN 2523-6784

In this case, it is intended that the black color corresponds to the background that surrounds the part of interest, while the white is assigned to the surface of the latter, highlighting it from the rest of the captured image. However, it is necessary to mention that, by submitting three different colors of the part to the analysis, three different options were determined for the identification of each color, which leads to distinguish one part from another by means of such an attribute.

Object segmentation

Segmentation divides a binarized image into various regions, by highlighting the object of interest from its background, with the aim of extracting its own features (Brosnan & Sun, 2004). Thus, for the purposes of the exposed analysis, the segmentation allows the proposal, by the user, of the maximum and minimum values per component of the RGB spectrum, for the distinction of the part from the rest of the image captured by the camera. For which, the gradual modification of each color component (red, green or blue) was performed; starting by removing those that do not suggest a great presence in the analyzed part. For the success of the aforementioned operation, within the algorithm, the visualization of the analyzed object was programmed on an alternate screen, once binarized, as well as a set of bars that allowed the user to directly modify the conditions for the segmentation of each part, according its color; as can be seen in figure 6. The slider bars used, whose values range from 0 to 255, indicate the shade of the color to be identified, from its lowest or darkest point to its highest or brightest point, depending on the primary component to be affected.

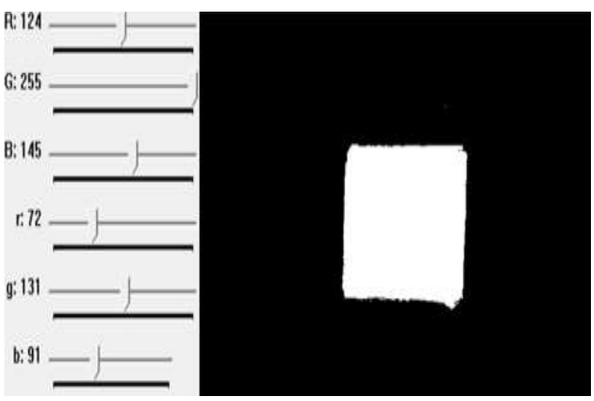

a) b)

Figure 6 Green part segmentation: *a)* proposed values and *b)* aspect
Source: Own Elaboration, 2022

This operation was applied differently for each part analyzed, since the levels proposed for the detection of a specific color would be dissimilar from those necessary for the recognition of any of the other two identifiable ones. Likewise, from the execution of an adequate operation, it can be ensured that if a part, with a different color, is placed near to another whose color has been previously segmented, the vision system ignores the attributes of the first. This effect is due to, as it does not belong to the segmented color group, the system interprets any other part as a portion of the background in the captured image.

It is worth mentioning that, if during the segmentation of any of the proposed class colors, an excessive withdrawal is exerted on any of their components, it is possible that there is a loss of substantial information in the analyzed part. Such a situation can lead to an inadequate interpretation of the information established by the processing, as shown in figure 7. In this figure, an incomplete determination of the area corresponding to the represented part can be seen, which would negatively affect the subsequent phases of the analysis performed.

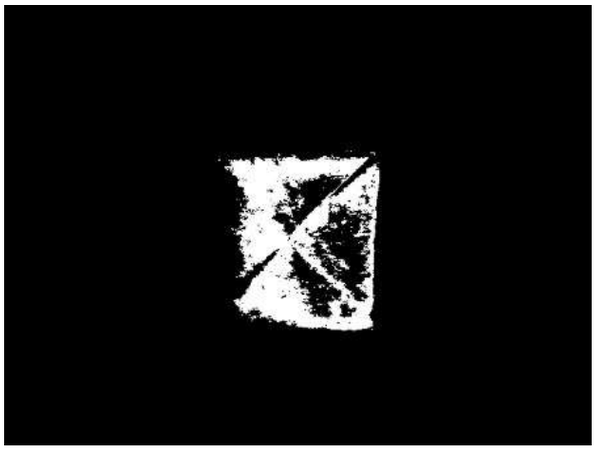

Figure 7 Loss of part information
Source: Own Elaboration, 2022

After completing the segmentation process on each specific class, within the initially proposed categorization, the quantities given in table 2 are determined, in which the minimum and maximum values respectively used to identify the color of the analyzed part are shown. It should be noted that the exclusive use of each pair of values allows the identification of parts with the indicated color, seeking at all times to eliminate possible overlaps between sets that lead to interpreting one color as another.

ISSN 2523-6784

Part Color	R Component		G Component		B Component	
	Min.	Max.	Min.	Max.	Min.	Max.
Red	183	255	83	160	87	163
Green	72	124	131	255	91	145
Blue	44	124	74	177	188	255

Table 2 Values set for color targeting
Source: Own Elaboration, 2022

Blurring operation

The blurring operation allows the smoothing of the edges that define an object analyzed in a specific uniform background. Therefore, if there are cavities or irregular regions in the captured object, which do not exist in the real part, they could well be eliminated by means of this operation, or at least they would acquire a more homogeneous appearance. Such an action is possible by averaging the colors of a specific pixel and some of its neighboring pixels (Du & Sun, 2004).

Thus, after performing the color identification process in each part analyzed, it is possible that, due to the excessive modification of some tonality index, isolated portions of color or noise that do not belong to the set of pixels that represent each detected part be noticed. Such a situation can be inherently caused by trying to preserve substantial information that allows the part to stand out from the background that surrounds it; being necessary the blurring of the captured image.

Dilation operation

Smoothing the edges of an object, from the blurring process, could result in an irregular entity that does not retain the shape, proportions, or sizing of the original part. Therefore, it is decided to increase the region of the analyzed object, by means of the dilation operation (Patel, Kar, Jha, & Khan, 2012). This operation would not only provide a solid and uniform appearance in the processed object, but also the cavities or hollows caused by previous operations can be eliminated, as they are "absorbed" by the action of dilation. Continuing the processing executed, the application of the dilation operation seeks, as much as possible, to generate a processed part with an appearance very similar to the original, which may be evident in the shape of the outer contour that distinguishes it from the background.

This limit between pixels of two different classes, will highlight the final contour of the processed part for its identification, not only of the background that surrounds it, but of other parts in different colors, which can be captured at the same time, by the camera, on the belt.

Part contour

Post-processing, feature extraction defines a set of attributes that meaningfully represent information that is important for analysis and classification of a studied object. The most commonly analyzed features are color, shape and texture (Patel, Kar, Jha, & Khan, 2012). Thus, feature selection algorithms base their function on the establishment of properties that allow adequately defining the attribute of interest for the study, which, after processing, can be located in the contour or region of the analyzed object (Makem, Ou, & Armstrong, 2012).

In this case, after establishing the region associated with the area occupied by the processed part, for each color, it was necessary to draw a contour that would fix the identified surface of the background or of some other part that could be captured by the camera. In addition, the customization of the established contour was done, based on the designation of a specific thickness and color; where the latter alluded to the color detected in the part captured in particular.

Part classification results

The formation of images through the camera used, as well as the application of techniques for their pre-processing, allowed to characterize each part of interest, based on its color, distinguishing it from the background, regardless of whether they were in motion. In particular, the function of segmentation in estimating the necessary parameters for the identification of each component of the RGB spectrum, present in each analyzed part, through binarization, is highlighted.

Thus, as a result of the segmentation, executed on each proposed class, it was possible to establish the quantities specified in table 2, which represent the minimum and maximum values necessary for the adequate identification of the color of each analyzed part.

ISSN 2523-6784

Therefore, the exclusive use of each pair of given values allows the characterization of the parts in the respective color, indicated in the table itself; considering the elimination of any overlap between tonal sets, which leads to interpreting a color as a different one.

It should be noted that, based on the given values, it was also possible to adequately identify each of the three possible color classes in an analyzed part, independently, even in the presence of objects belonging to the remaining classes. Such an effect can be verified in figure 8, in which a respective part of each class is characterized, close to elements corresponding to the other two analyzed, without this fact affecting the effectiveness of the identification task, depending on the color.

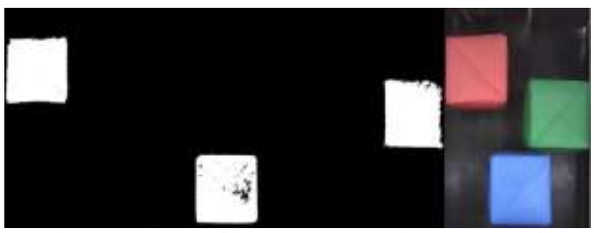

a) *b)* *c)* *d)*

Figure 8 Segmentation by class: a) red, b) blue, c) green and d) acquired image
Source: Own Elaboration, 2022

It is noteworthy that, during the part recognition process, efforts were made to have significant information available that would enable a propitious definition, not only of its color, but also of its physical dimensions; which were particularly related to the region detected for each one. Therefore, the application of blurring and dilation operations was a priority, in order to have an area as uniform as possible, which would represent each part analyzed, and in turn, its limits with respect to the background, as can be seen in the figures 9 and 10, respectively.

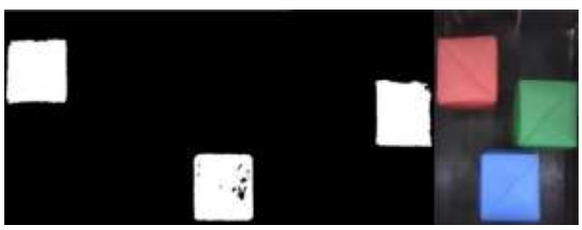

a) *b)* *c)* *d)*

Figure 9 Blurring by class: a) red, b) blue, c) green and d) acquired image
Source: Own Elaboration, 2022

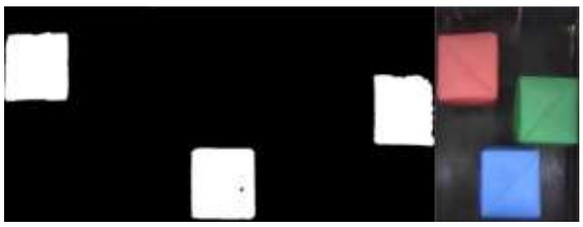

a) *b)* *c)* *d)*

Figure 10 Dilation by class: a) red, b) blue, c) green and d) acquired image
Source: Own Elaboration, 2022

Resuming the identification of parts of a specific class in the presence of those that belonged to a different one, figure 11 shows the imposition of an external contour on each analyzed part. This contour encloses the region that represents the area identified in each part, determined by a set of pixels that share the same color. Finally, figure 12 exhibits the adequate identification of a part for each color, once it describes a movement through the conveyor belt. It is noted that despite the appearance of noise, inherent to the given displacement, the recognition of each part is performed successfully.

a) *b)* *c)* *d)*

Figure 11 Contour by class: *a)* red, *b)* blue, *c)* green and *d)* acquired image
Source: Own Elaboration, 2022

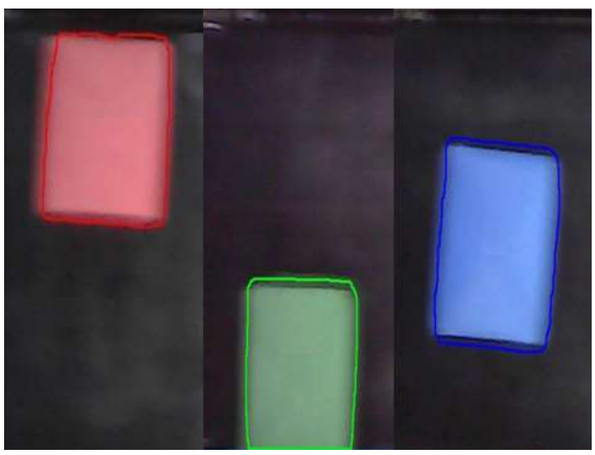

a) *b)* *c)*

Figure 12 Moving part classification: a) red, b) green and c) blue
Source: Own Elaboration, 2022

ISSN 2523-6784

Conclusions

Through the acquisition of images and their processing, vision systems enable the recognition of features that are of interest for the execution of specific tasks, commonly the identification and classification of parts. Such functions are especially enhanced when they are performed on parts that prescribe a continuous movement, as analyzed by this work. However, the dynamism provided to the detection process implies a timely solution to inconveniences that may arise, such as: the appearance of noise, the generation of shadows or the formation of clusters of pixels in areas outside the object of interest.

Thus, the mitigation of the negative effects caused by the movement of the studied parts must be sought from the preprocessing phases in order to avoid, as far as possible, the substantial loss of relevant features and, therefore, the inadequate interpretation of the information obtained from the operation itself.

Although, beforehand, it is essential to have adequate lighting to reduce the occurrence of alterations in the capture of a part, which affect negatively its subsequent treatment. Therefore, an effective conduction between the capture of an image and its processing, leads to guaranteeing the full identification of the attributes of interest; as observed in the developed process.

It should be noted that, within the preprocessing, the segmentation operation serves as the basis for the suitable estimation of the pixel region associated with each analyzed part. In this case, the identification and application of the values of the color components in the effective distinction of each class, with respect to another also scrutinized, even in its presence, was a great success; as seen in the reported results.

Even so, the contribution of the blurring and dilation operations, also performed, is not underestimated, since they strengthened the subsequent recognition function, by improving the description of the established regions where the segmentation function was limited, such as gaps and irregularity on the edges.

In this way, and given the operating results obtained from the test of the implemented vision system, the competitiveness achieved by it is validated, even in the case of a prototype. Also noteworthy is the quality of the task performed, through the use of low-cost, easy acquisition and simple handling devices; as well as the development of the required programming, based on open-source software and libraries, which were executed from a personal computer. It should be noted that the functionality achieved can be comparable to that provided by dedicated systems, which are commonly expensive and require a large amount of processing resources.

References

Ayub, M. A., Mohamed, A. B., & Esa, A. H. (2014). In-line inspection of roundness using machine vision. *Procedia Technology*, 807-816. doi:10.1016/j.protcy.2014.09.054

Barari, A. (2013). Inspection of the machined surfaces using manufacturing data. *Journal of Manufacturing Systems*, 107–113. doi:10.1016/j.jmsy.2012.07.011

Bozma, H. I., & Yalçın, H. (2002). Visual processing and classification of items on a moving conveyor: A selective perception approach. *Robotics and Computer-Integrated Manufacturing*, 125-133. doi:10.1016/S0736-5845(01)00035-7

Brosnan, T., & Sun, D.-W. (2004). Improving quality inspection of food products by computer vision - A review. *Journal of Food Engineering*, 3-16. doi:10.1016/S0260-8774(03)00183-3

Dowlati, M., de la Guardia, M., & Mohtasebi, S. S. (2012). Application of machine-vision techniques to fish-quality assessment. *TrAC Trends in Analytical Chemistry*, 168-179. doi:10.1016/j.trac.2012.07.011

Du, C.-J., & Sun, D.-W. (2004). Recent developments in the applications of image processing techniques for food quality evaluation. *Trends in Food Science & Technology*, 230-249. doi:10.1016/j.tifs.2003.10.006

ISSN 2523-6784

Jackman, P., & Sun, D.-W. (2013). Recent advances in image processing using image texture features for food quality assessment. *Trends in Food Science & Technology*, 35-43. doi:10.1016/j.tifs.2012.08.008

Kodagali, J. A., & Balaji, S. (2012). Computer vision and image analysis based techniques for automatic characterization of fruits - A review. *International Journal of Computer Applications*, 1-14. doi:10.5120/7773-0856

Makem, J. E., Ou, H., & Armstrong, C. G. (2012). A virtual inspection framework for precision manufacturing of aerofoil components. *Computer-Aided Design*, 858-874. doi:10.1016/j.cad.2012.04.002

Patel, K. K., Kar, A., Jha, S. N., & Khan, M. A. (2012). Machine vision system: A tool for quality inspection of food and agricultural products. *Journal of Food Science and Technology*, 123-141. doi:10.1007/s13197-011-0321-4

Santos-Gomes, J. F., & Rodrigues-Leta, F. (2012). Applications of computer vision techniques in the agriculture and food industry: A review. *European Food Research and Technology*, 989-1000. doi:10.1007/s00217-012-1844-2

Selver, M. A., Akay, O., Alim, F., Bardakçı, S., & Ölmez, M. (2011). An automated industrial conveyor belt system using image processing and hierarchical clustering for classifying marble slabs. *Robotics and Computer-Integrated Manufacturing*, 164-176. doi:10.1016/j.rcim.2010.07.004

Tavakoli, M., & Najafzadeh, M. (2015). Application of the image processing technique for separating sprouted potatoes in the sorting line. *Journal of Applied Environmental and Biological Sciences*, 223-227. doi:10.13140/2.1.2093.0887

Tran, H. N. (2019). Study on image processing method to classify objects on dynamic conveyor. *Science & Technology Development Journal-Engineering and Technology*, 127-136. doi:10.32508/stdjet.v2iSI2.489

Vijayarekha, K. (2012). Machine vision application for food quality: A review. *Research Journal of Applied Sciences, Engineering and Technology*, 5453-5458. Obtenido de https://maxwellsci.com/print/rjaset/v4-5453-5458.pdf

Wang, H., Wang, J., Chen, W., & Xu, L. (2018). Automatic illumination planning for robot vision inspection system. *Neurocomputing*, 19-28. doi:10.1016/j.neucom.2017.05.015

Wu, D., & Sun, D.-W. (2013). Colour measurements by computer vision for food quality control - A review. *Trends in Food Science & Technology*, 5-20. doi:10.1016/j.tifs.2012.08.004

Xiao-bo, Z., Jie-wen, Z., Yanxiao, L., & Holmes, M. (2010). In-line detection of apple defects using three color cameras system. *Computers and Electronics in Agriculture*, 129-134. doi:10.1016/j.compag.2009.09.014

Ye, X. W., Dong, C. Z., & Liu, T. (2016). A review of machine vision-based structural health monitoring: Methodologies and applications. *Journal of Sensors*, 1-10. doi:10.1155/2016/7103039

Zhang, B., Huang, W., Li, J., Zhao, C., Fan, S., Wu, J., & Liu, C. (2014). Principles, developments and applications of computer vision for external quality of fruits and vegetables: A review. *Food Research International*, 326-343. doi:10.1016/j.foodres.2014.03.012

ISSN 2523-6784

Article **Journal of Systematic Innovation**
June 2022 Vol.6 No.18 11-18

Mathematical analysis for the selection of the heating equipment of the hot forming stamping

Análisis matemático para la selección del equipo de calentamiento del proceso de estampado en caliente

HUERTA-GÁMEZ, Héctor†*, CERRITO-TOVAR, Iván de Jesús, PÉREZ-PÉREZ, Arnulfo and TORRES-MENDOZA, Raymundo Esteban

Universidad Politécnica Juventino Rosas, Departamento de Ingeniería en Sistemas Automotrices.Hidalgo 102, Comunidad de Valencia, Juventino Rosas, Gto, México.

ID 1st Author: *Héctor, Huerta-Gámez* / **ORC ID:** 0000-0002-5088-310X, **CVU CONACYT ID:** 373690

ID 1st Co-author: *Iván de Jesús, Cerrito-Tovar* / **ORC ID:** 0000-0002-8601-9911

ID 2nd Co-author: *Arnulfo, Pérez-Pérez* / **ORC ID:** 0000-0001-6354-8899, **CVU CONACYT ID:** 176434

ID 3rd Co-author: *Raymundo Esteban, Torres-Mendoza* / **ORC ID:** 0000-0001-8493-6946

DOI: 10.35429/JSI.2022.18.6.11.18 Received March 14, 2022; Accepted June 29, 2022

Abstract

This article shows the mathematical development to determine the length and cycle time of a furnace that is used for heating parts in the hot forming process. The input parameters, the required production capacity and the temperature to reach the austenite phase in the material were used. For the mathematical process, it was necessary to know the stages for the process, considering that there are two methods: the direct and indirect process. Subsequently, the number of annual pieces that should be produced per year was determined, thereby being able to conclude the cycle time that should be estimated for the furnace; Likewise, some thermal parameters that the oven must have were known, such as the internal temperature, which helped to know its length, in order to meet the demands of the production volume. This work aims to present alternatives to the industries dedicated to the stamping process, specifically hot forming stamping, based on the analysis of the selection of the heating equipment, based on the production needs.

Stamping, Development, Mathematical

Resumen

El presente artículo muestra el desarrollo matemático llevado a cabo para determinar la longitud y el tiempo ciclo de un horno que es usado para el calentamiento de piezas que son sometidas a un proceso de estampado en caliente. Como parámetros de entrada se usó la capacidad de producción requerida y la temperatura para alcanzar la fase de austenita en el material. Para llevar a cabo el desarrollo matemático, fue necesario conocer las etapas del proceso, considerando que existen dos métodos para realizarlo, como son: el proceso directo e indirecto. Posteriormente se determinó la cantidad de piezas anuales que se deberían de producir por año, con ello poder concluir el tiempo ciclo que se debe estimar para el horno; también se conocieron algunos parámetros térmicos que debe poseer el horno, como son la temperatura interna, la cual ayudó a conocer la longitud del mismo, con la finalidad de que cumpla con las exigencias del volumen de producción. Con este trabajo se pretende ampliar el panorama a las industrias dedicadas al proceso de estampado, específicamente del estampado en caliente, lo anterior basado en el análisis de la selección del equipo de calentamiento, a partir de las necesidades de producción.

Estampado, Desarrollo, Matemático

Citation: HUERTA-GÁMEZ, Héctor, CERRITO-TOVAR, Iván de Jesús, PÉREZ-PÉREZ, Arnulfo and TORRES-MENDOZA, Raymundo Esteban. Mathematical analysis for the selection of the heating equipment of the hot forming stamping. Journal of Systematic Innovation. 2022. 6-18: 11-18

* Correspondence to Author (e-mail: hhuerta_ptc@upjr.edu.mx)
† Researcher contributing as first author.

1. Introduction

Technological progress within the production sector has led industries to have equipment with greater capacities to carry out the tasks entrusted to them.

Within the automotive sector is the forming of parts, in which there are a series of equipment with which they work, among which are the heating furnaces.

Raising the temperature of the part to be worked on is of vital importance, as it depends on it to have the right microstructures, and consequently, to be able to have the mechanical properties that are sought in the part.

The main objective of the hot stamping process is to develop parts with high impact resistance (up to 1600MPa), but with very thin part thicknesses (up to 2mm).

In this work, an analysis of the furnace capacity will be carried out, which must meet the production volume requirements set by the production sector.

The work is considered to be carried out through a sequence of steps, which will lead to fulfil the objective.

The article initially proposes a methodology based on the particular needs of the project. Subsequently, in the development, the stages of hot stamping by the direct method and the indirect method are described. Within this same section, the chemical composition is shown, as well as some of the thermal properties of the material to be heated. The behaviour of the emissivity property of the material with respect to temperature is also reviewed in order to determine an adequate heating time, considering equations that involve the production volume; likewise, as a viable alternative to determine the heating time, the heating speed of the part will be known.

In the results section, the cycle time of the furnace can be observed, as well as the length of this (furnace), which is the end point of the project. Finally, there will be a conclusion of the work, where it will be reviewed if the objective was fulfilled, and consequently, the improvements that can be carried out will be commented.

Methodology to be developed

The success or failure of a project is based on the adequate design of a methodology to be followed, which must be adjusted to the characteristics and needs of the project, in order to achieve the proposed goal. The methodology carried out in this project is shown in Figure 1, in which it can be seen that the objective of the project was considered as important points, as well as the estimated production volumes over the course of a year.

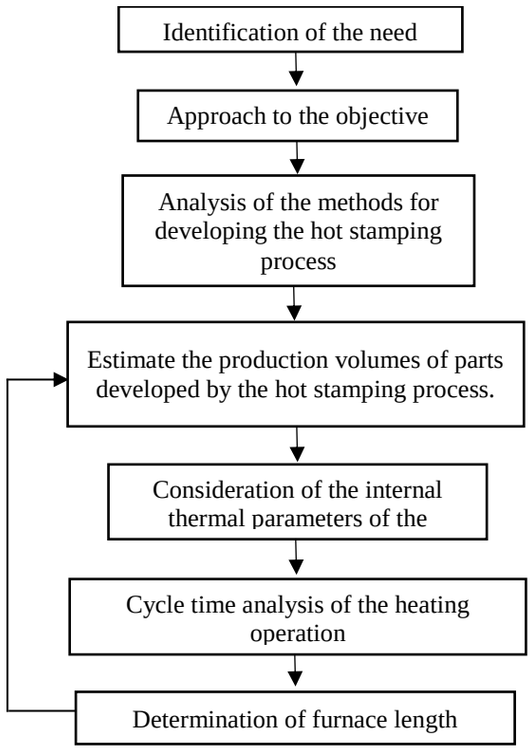

Figure 1 Methodology
Source: Own Elaboration

Development

Consideration of the analysis of the study

Before starting the analysis and development of the process, it is important to comment that the study carried out in this work only contemplates the phenomenon of heat transfer by radiation. In studies carried out on this type of furnace, the 3 types of heat transfer mechanisms were considered: conduction, convection and radiation, at different temperatures between the furnace and the workpiece, with radiation as the dominant heat transfer mechanism (Dvorak, Tawk and Vít, 2016).

ISSN 2523-6784

Methods for carrying out the hot stamping process

To further understand the importance of the furnace as a necessary element in the part forming process, it is necessary to understand the hot stamping methodology.

The stamping process involves a sequence of steps in which small parts, known as sheets, are formed. This process uses dies, presses, among others, as common elements.

Unlike conventional stamping, the hot stamping process uses heat as a support to obtain the mechanical properties required by the elements that are subjected to high impacts, high stresses, among others.

The hot stamping process can be carried out in two different ways:

Direct method

In the direct method of the Hot Forming Stamping (HFS) process (Figure 2), the sheet is brought to a temperature between 900°C and 950°C to obtain an austenite microstructure, then transferred to the die where the form is made, followed by cooling through a heat transfer unit. At temperatures above 700°C, the material can be handled excellently, so that it can take the shape that the die has. The stamping is carried out on the foil and cooled under pressure for a certain time, according to the thickness of the foil. During this period the stamped part is cooled at speeds ranging from 50 to 100 °C/s by circulating water, thus obtaining the ideal microstructure.

Finally, the stamped part leaves the hot stamping line at around 150 °C and with it excellent mechanical properties: tensile strength of 1,400 to 1,600 MPa (around 200 to 230 KSI), as well as a yield strength between 1,000 and 1,200 MPa (around 145 to 175 KSI).

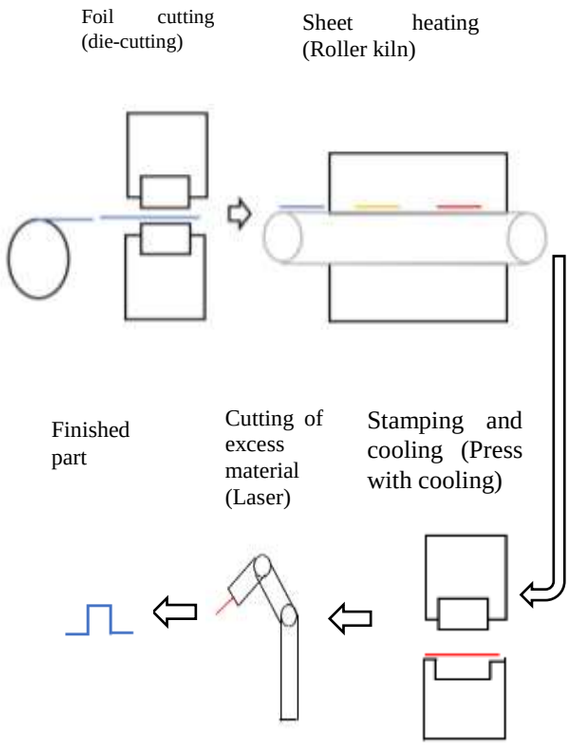

Figure 2 Direct method of the HFS process
Source: Own Elaboration

Indirect method

Unlike the direct process, the indirect hot stamping process has an additional operation called preforming (no heat is added in this operation), in which 90% to 95% of the final shape is formed. The preformed part is then heated to austenitising temperature (approximately 950 °C) in a continuous furnace, and the final shape is then made, in addition to cooling inside the press (Figure 3).

Having known the hot stamping process by the direct and indirect methods, we proceeded to know the type of steel that can be worked by this process, knowing that the sheet material must be a boron steel to work hot and thus be able to obtain the necessary properties.

The materials commonly used for the hot stamping process are boron steels, since, due to their mechanical properties, after hot stamping, they are positioned within the range of steels developed to meet the demands required by vehicle assemblers.

ISSN 2523-6784

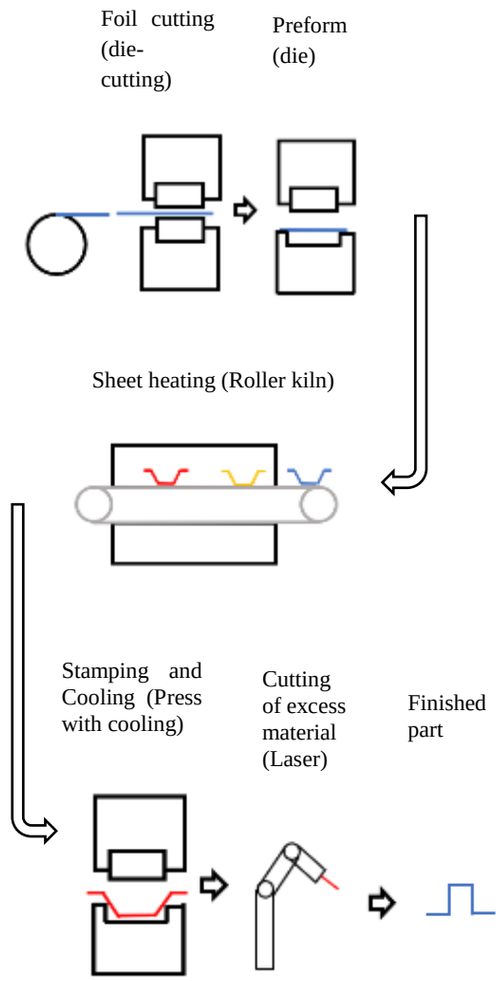

Figure 3 Indirect method of the HFS process
Source: Own Elaboration

Table 1 shows the chemical composition of boron steels (Ganapathy et al., 2019), which are used for the hot stamping process, specifically refers to 22MnB5 steel.

Component	% of composition
C	0.20
Mn	1.17
Si	0.25
Cr	0.20
S	0.002
B	0.0029
Ti	0.028
Nb	0.001
Ni	0.023

Table 1 Chemical composition of boron steel
Source: Own Elaboration

The analysis of the heating time depends on the thermal properties of the material, among which are: density, heat capacity, thermal conductivity (Shapiro, 2009), which are shown in Table 2:

Thermal property	Quantity
ρ,density (kg/m^3)	7830
C_p,heat capacity $(J/kg*K)$	650
k,thermal conductivity $(W/m*K)$	32
λ,latent heat , (kJ/kg)	58.5

Table 2 Thermal properties of boron steel
Source: Own Elaboration

During the hot forging process, the material undergoes microstructural changes, which are described below:

At the beginning of the process, the material has a ferritic-perlitic microstructure with a tensile strength of 600 MPa. It enters the furnace to be heated to a temperature between 900 °C and 950 °C, as a result of which the microstructure changes to austenite. It is then transferred to the press, where it reaches a temperature between 650 °C and 850 °C, the part is shaped and quenched in order to obtain a martensitic microstructure and a strength of 1600 MPa.

Figure 4 shows the microstructural changes during the hot stamping process, from the time it enters the furnace until it leaves the stamping station.

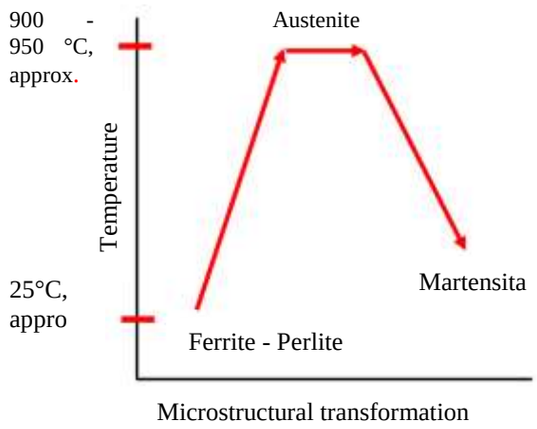

Figure 4 Microstructural changes within the HFS process
Source: Own Elaboration

3.4 Heating-up time of the workpiece

The heating time plays an important role in the selection of the furnace, as the size required for the furnace depends to a large extent on this, as well as the production volume. Also, within the equations, the volume of the part being worked on is considered, so it is necessary to know its geometric dimensions.

ISSN 2523-6784

The part that will be taken as a parameter is the lateral reinforcement of the vehicle, for which the sheet will be considered to be 1.4m long by 0.6m wide, as well as a thickness of 1.5mm (Figure 5):

Figure 5 Dimensions of the working sheet
Source: Own Elaboration

For the determination of this time, some thermal parameters were considered, among which are: temperature inside the furnace, the temperature of the film and the emissivity (Dvorak, Tawk and Vít, 2016); the above data can be seen in Table 3.

Temperature inside the oven	°C	930	930	930
Film temperature	°C	25	600	900
Emissivity	(1)	0.38	0.11	0.54
Convection heat transfer coefficient	(W m^{-2} K^{-1})	9.50	5.60	4.10
Radiation heat flux	(W m^{-2})	44.96	9.44	6.16
Convection heat flux	(W m^{-2})	8.6	1.85	0.12

Table 3 Chemical composition of boron steel
Source: Own Elaboration

As can be seen in Table 2, emissivity is a function of temperature, and therefore of time. It can also be seen that the heat flow by radiation is the parameter that has the greatest effect on the part to be heated, so the geometry that describes the behaviour of emissivity with respect to temperature was determined (Figure 6).

The geometrical locus shown in Figure 6 can be described in mathematical terms by Equation 1:

$$\varepsilon = 2.175x10^{-6}T^2 - 1.83x10^{-3}T + 0.424 \quad (1)$$

Where:

ε = Emissivity
T = Temperature in °C

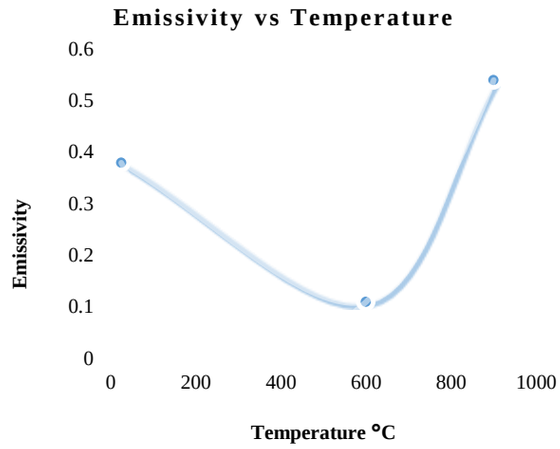

Figure 6 Behaviour of emissivity vs temperature
Source: Own Elaboration

Equation 4 provided an approximation of the emissivities at different temperatures, with which it is possible to determine the total time the workpiece would spend in the furnace. Table 4 shows the emissivities inside the furnace at various temperatures:

Temperature (°C)	Emissivity
25	0.37961
100	0.26275
200	0.145
300	0.07075
400	0.04
500	0.05275
600	0.109
700	0.20875
800	0.352
900	0.53875

Table 4 Emissivities at various temperatures
Source: Own Elaboration

Equation 2 (Incropera & Dewitt, 1999) was used to determine the heating time as a function of emissivity and temperatures:

$$\rho Vc\frac{dT}{dt} = -\sigma\varepsilon A(T^4 - T_\infty^4) \quad (2)$$

Solving the differential equation between the limits (T=T_i @t=0) and (T=T @ t), we obtain Equation 3 (Incropera & Dewitt, 1999):

$$t = \frac{\rho Vc}{4A\sigma\varepsilon T_{alr}^3}\left[\ln\left|\frac{T_{alr}+T}{T_{alr}-T}\right| - \ln\left|\frac{T_{alr}+T_i}{T_{alr}-T_i}\right| + 2\left(\tan^{-1}\frac{T}{T_{alr}} - \tan^{-1}\frac{T_i}{T_{alr}}\right)\right] \quad (3)$$

ISSN 2523-6784

Where:

V is the volume of the part to be heated.
A is the contact surface of the radiation phenomenon.
σ is the Stefan-Boltzman constant ($5.67x10^{-8}\ W/m^2 * K^2$
$T_{alr}$is the temperature inside the furnace.
T_i is the initial temperature of the workpiece to be heated.
T is the final temperature of the workpiece to be heated.

Equation 3 applies when the relationship given by equation 4 (Incropera & Dewitt, 1999) is fulfilled:

$$Bi = \frac{hL_c}{k} < 0.1 \quad (4)$$

Where:

Bi is the Biot number which is a dimensionless quantity.
h is the convective heat transfer coefficient.
$L_c$is the critical length, in practical cases it is considered as the thickness.

Equation 5 (Incropera & Dewitt, 1999) is used to obtain Lc:

$$L_c \equiv {}^{V}/_{A} \quad (5)$$

On the other hand, it has been reviewed in some references that the heating time can be determined from controlled speeds, i.e. a heating speed of around 7.5 °C/s has been considered until a temperature of 750 °C is reached, then the speed is decreased from 7.5 °C/s to 1°C/s, this last speed is managed until 900°C, afterwards the temperature of 900°C is maintained for a lapse of 1 minute (Dvorak, Tawk and Vít, 2016), the above study was developed for 1.5mm thick sheets.

3.5 Production volume

To determine the number of parts per day, Equation 6 is used:

$$\text{No. of pcs/day} = \frac{{}^{\text{Pcs}}/_{year}}{{}^{\text{days}}/_{\text{year (working days)}}} \quad (6)$$

Equation 7 was used to determine the number of parts per hour:

$$\text{No. of pcs/hour} = \frac{{}^{\text{Pcs}}/_{\text{day}}}{{}^{\text{hours}}/_{\text{day (working days)}}} \quad (7)$$

To determine the cycle time, Equation 8 was considered:

$$\text{t}_{\text{cicle}} = \frac{3600}{\text{No.of pcs/hour}} \quad (8)$$

Equation 9 describes the appropriate length for the furnace, which refers to the total distance the part will travel from entering at room temperature to leaving at austenitising temperature (Figure 7); this length is a function of the heating time, the cycle time and a term called "Llote", which is the length that a "group" of parts spans. The "Llote" can cover 1 part, 2 parts or more (Figure 8), as it will depend on the number of robots that are between the heating operation and the forming operation, as well as the cycle time that is handled in the latter.

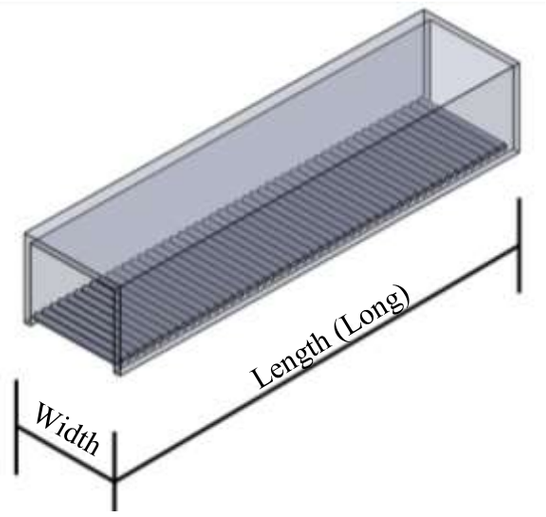

Figure 7 Furnace length
Source: Own Elaboration

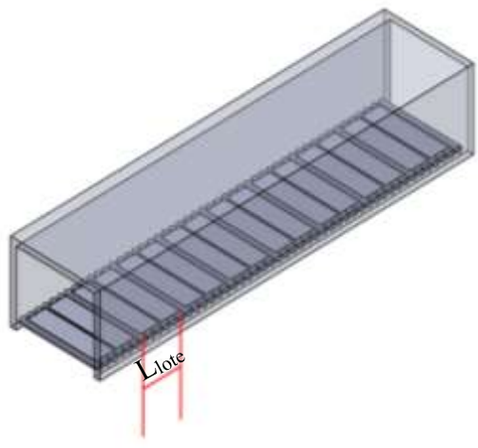

Figure 8 Description of the term Llote
Source: Own Elaboration

ISSN 2523-6784

$$L_{Oven} = \frac{t_{heating}}{t_{cicle}}(L_{lote}) \quad (9)$$

3. Results

Two methods were used to determine the heating time:

1. By taking into account the following properties of the material to be heated:

$\rho = 7830\ {}^{Kg}/_{m^3}$

$C_p = 650\ {}^{J}/_{Kg.K}$

$V = 1.26x10^{-03} m^3$

$A = 0.84 m^2$

$\sigma = (5.67x10^{-08})$

$T_{alr} = 930°C$

$T_i = 25°C$

$T = 950°C$

as well as the emissivities at the different temperatures, a total heating time of:

$t_{heating} = 345.66\ s$

2. Considering the option in which the part is heated at 7°C/s until it reaches a temperature of 750°C, then heated at a rate of 1°C/s until it reaches 900°C, finally left at 900°C for one minute, we have a heating time:

$t_{eating} = 313.57\ s$

In order to determine the cycle time of the production line, the following considerations were made:

For a total of 500,000 pcs/year.

This production volume is considering that the part being analysed is a lateral reinforcement, which is found on both sides of the vehicle.

Taking as a given that 240 days per year (working days) are worked, Equation 6 was used, so it was obtained that:

$$\text{No. of pcs/day} = 2083\ {}^{Pcs}/_{day}$$

To determine the number of parts per hour, Equation 7 was used, with the necessary data in addition to the consideration that in a working day 21 hours are worked (time at 100%) the following was obtained:

$$\text{No. of pcs/hour} = 100\ {}^{Pcs}/_{hour}$$

In order to determine the cycle time of the furnace, Equation 8 was considered, giving a cycle time equal to:

$t_{cicle} = 36\ {}^{s}/_{Pza}$

Finally, the furnace length was obtained from Equation 9. Based on the two heating times determined, the cycle time and the area of the parts, as well as Llote = 1.4 m, the corresponding results are shown in table 5:

$T_{Heating}$ (s)	L_{Oven} (m)
345.66	13.4
313.57	12.2

Table 5 Furnace length in relation to heating time
Source: Own Elaboration

3. Conclusions

For practical purposes and quick and accurate results, the analysis can be considered only taking into account the controlled heating rate, since, due to the results obtained, the heating times are close.

Taking as a reference what exists commercially, the furnace should have a length of 15m and a width of 2m, with these dimensions, as well as an internal temperature that can reach at least 930°C, also taking into account the thermal conditions mentioned within the development, the production volume will be guaranteed. On the other hand, in order to contribute to the research on the analysis of the heating time, as well as to compare the results obtained in this work, an analysis of heating times can be proposed from the study of the microstructural changes as a function of time and temperature, considering the effect of the alloy components of the material.

ISSN 2523-6784

4. Acknowledgements

To the Universidad Politécnica Juventino Rosas (UPJR), specifically to the department of Automotive Systems Engineering (ISA) for the time given to the development of the project.

The current project did not require funding from the organisation, due to the scope and needs of the project.

5. References

Dvorak, B., Tawk, J.J. & Vít, T., 2016. Advanced Design of Continuous Furnace for Hot Stamping Line. Advanced High Strength Steel and Press Hardening, pp. 611 - 619. China: World Scientific. https://doi.org/10.1142/9789813140622_0097

Ganapathy, M., Li, N., Lin, J., Abspoel, M. and Bhattacharjee, D., 2019. Experimental investigation of a new low-temperature hot stamping process for boron steels. The International Journal of Advanced Manufacturing Technology, 105(1-4), pp.669-682. https://doi.org/10.1007/s00170-019-04172-5

Incropera, F. & Dewitt, D.,1999. Fundamentos de Transferencia de Calor (4a ed). Pearson Educación.

Shapiro, A., 2009. Finite Element Modeling of Hot Stamping. Metal Forming, 80, p. 658. https://doi.org/10.2374/SRI08SP065

ISSN 2523-6784

Article **Journal of Systematic Innovation**
June 2022 Vol.6 No.18 19-26

Analysis and dynamic simulation of the cardan shaft for the minilow prototype vehicle

Análisis y simulación dinámica del eje cardán para vehículo prototipo mini baja

AGUILAR-MORENO, Antonio Alberto†, GARCIA-DUARTE, Oscar Enrique*, ARELLANO-PATIÑO José Antonio and ALVAREZ-GARCIA, Eduardo

Universidad Politécnica de Juventino Rosas. Carrera de Ingeniería en Sistemas Automotrices. Hidalgo 102, Comunidad de Valencia, Juventino Rosas, Gto, México.

ID 1st Author: *Antonio Alberto, Aguilar-Moreno* / **ORC ID:** 0000-0002-7652-5925, **CVU CONACYT ID:** 254188

ID 1st Co-author: *Oscar Enrique, García-Duarte* / **ORC ID:** 0000-0002481-8438, **CVU CONACYT ID**: 290387

ID 2nd Co-author: *José Antonio, Arellano-Patiño* / **ORC ID:** 0000-0002-6402-6352

ID 3rd Co-author: *Eduardo, Álvarez-García* / **ORC ID:** 0000-0001-9372-5489

DOI: 10.35429/JSI.2022.18.6.19.26 Received March 14, 2022; Accepted June 29, 2022

Abstract

This article shows the finite element analysis for the simulation of dynamic loads to two prototype models of cardan shafts considering two types of material, alloy steel and 1045 steel, to determine the structural efficiency of work, by means of contour conditions extracted from two types of engines raised for a minilow vehicle. In order to perform the structural simulation of dynamic loads, it was essential to simulate motion analysis and determine that both models do not present some gap or energy irregularity. This consisted in obtaining the dynamic results (displacement and angular speed, torque and power), comparing them with those indicated by the manufacturer of each engine. The finite element analysis was then performed for the structural simulation of dynamic loads, identifying the element that generates the minimum Von Mises forces, the lowest unit displacement and the minimum safety factor. The aim of this work is to confirm whether the two models comply with the structural analysis of dynamic loads and, based on this, to select the one with the most favorable results to work on the transmission of a minilow car.

Analysis, Dynamic, Structural, Simulation, Efficiency

Resumen

El presente artículo muestra el análisis de elemento finito para la simulación de cargas dinámicas a dos modelos prototipo de ejes cardán considerando dos tipos de material, acero aleado y acero 1045, para determinar la eficiencia estructural de trabajo, mediante condiciones de contorno extraídas de dos tipos de motores planteados para un vehículo minibaja. Para realizar la simulación estructural de cargas dinámicas, fue imprescindible simular análisis de movimiento y determinar que ambos modelos no presenten algún desfase o irregularidad energética, lo cual consistió en obtener los resultados dinámicos (desplazamiento y velocidad angular, torque y potencia), comparándolos con los indicados por el fabricante de cada motor. Posteriormente se realizó el análisis de elemento finito para la simulación estructural de cargas dinámicas, identificando el elemento que genere los mínimos esfuerzos de Von Mises, el menor desplazamiento unitario y el mínimo factor de seguridad. En este trabajo se tiene como objetivo corroborar si los dos modelos cumplen con el análisis estructural de cargas dinámicas y en base a ello seleccionar el que comprenda con los resultados más favorables para trabajar en la transmisión de un auto minibaja.

Análisis, Dinámico, Estructural, Simulación, Eficiencia

Citation: AGUILAR-MORENO, Antonio Alberto, GARCIA-DUARTE, Oscar Enrique, ARELLANO-PATIÑO José Antonio and ALVAREZ-GARCIA, Eduardo, Analysis and dynamic simulation of the cardan shaft for the minilow prototype vehicle Journal of Systematic Innovation. 2022. 6-18: 19-26

* Correspondence to Author (e-mail: ogarcia_ptc@upjr.edu.mx)
† Researcher contributing as first author.

Introduction

BAJA SAE is an event for undergraduate engineering students, organised by the Society of Automotive Engineers. The event organised on behalf of the MiniBAJA competition serves as a platform for young engineering students to showcase their skills by designing, manufacturing and validating a single-seater off-road vehicle and gain real-life experience while overcoming obstacles and challenges. (HUERTA-GAMEZ *et al*., 2020).

The automotive drivetrain system is designed to handle the power generated by an internal combustion engine and deliver it directly to the rear wheels for rear-wheel drive vehicles. One of the most important mechanical elements that assists the transmission of power, torque and speed is the cardan shaft, which generally comprises a drive shaft, as well as crossheads and flanges that help to optimise the transfer of these mechanical forces, to name the most prominent ones (Ciornei *et al*., 2019).

The cardan shaft is the main element to transmit the engine power, therefore, the study of two models of cardan shaft for a minibox vehicle will be carried out. This analysis will be developed based on a structural simulation of motion loads with materials added to the models, such as alloy steel and 1045 steel and with two different types of selected engines, which will provide results for interpretation in dynamic and finite element structural analysis plots.

Motors used

The cardan shafts will be subjected to the simulation study by means of two motors, simulating the work, power and angular velocity they provide, observing the behaviour of the proposed shaft models.

The engines were selected under the criteria of the SAE regulation 2022 formula, which indicates that they must be four-stroke and less than or equal to 710 cc per cycle. The first engine selected is the Blue Core 4-stroke, forced air-cooled SOHC single-cylinder engine and the second is the CBF125 twister 4-stroke, SOHC 2-valve single-cylinder engine; the characteristics of both engines are shown in Table 1.

Technical specifications		
Engine	Blue Core	CBF125 TWISTER 2022
	4-stroke	4-stroke
	Single-cylinder	Single-cylinder
	SOHC	SOHC
	2-valve	2-valve
Maximum Power	11.9 Hp at 7500 RPM	8.5 Hp at 7000 rpm
Maximum Torque	12.8 N-m at 4500 RPM	10.1 N-m at 5000 rpm
Displacement	149 cc	124.7 cc
Transmission	5-speed return type	4-speed return type
Cooling System	Forced air	Forced air

Table 1 Engine characteristics
Source: Own Elaboration (Word)

Material used

The selection of the appropriate material is an important point to consider, as the results of the simulation will depend on it. Table 2 shows the materials used in the simulation, which are adjusted to the boundary conditions to which the cardan shaft will be subjected, such as power and torsion according to the analysis of the movement in the structural element.

Material	Alloy Steel	AISI-1045 steel	Symbol
Property	Value	Value	Units
Modulus of elasticity	210000	205000	N/mm^2
Poisson's ratio	0.28	0.29	N/D
Shear modulus	79000	80000	N/mm^2
Bulk density	7700	7850	kg/m^3
Tensile limit	723.8256	625	N/mm^2
Elastic limit	620.422	530	N/mm^2
Coefficient of thermal expansion	1.30E-05	1.15E-05	/K
Thermal conductivity	50	49.8	W/(m·K)
Specific heat	460	486	J/(kg·K)

Table 2 Mechanical properties of steels
Source: Own Elaboration (Word)

Two steel type materials were selected, alloy steel, due to its high carbon content and 1045 steel, the latter contains a lower percentage of carbon, however, it is frequently used for gear systems, bolts, transmission shafts, among other uses of high structural grade.

Figure 1 shows the parameters of the automotive cardan shaft. The basic length is 932 mm, while the outer diameter is 80 mm, and the inner diameter is 60 mm.

ISSN 2523-6784

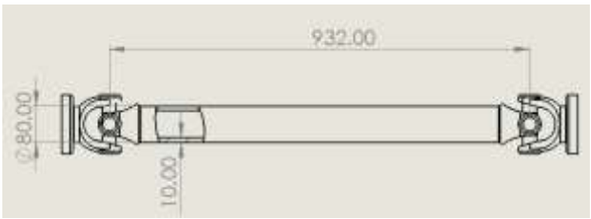

Figure 1 Geometric properties of the automotive cardan shaft
Source: Own Elaboration (Solidworks)

Figure 2 shows the parameters of the cardan shaft for a motor trolley. The basic length is 770.23 mm, while the outer diameter is 85 mm, and the inner diameter is 70 mm.

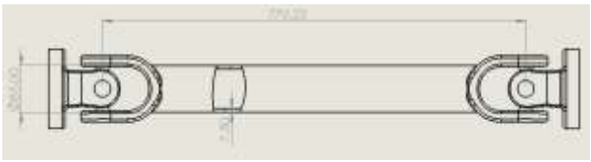

Figure 2 Geometrical properties of the trolley motor drive shaft
Source: Own Elaboration (Solidworks)

Analysis

After selecting the two engines, the Blue Core and the CBF125 Twister 2022, as well as the two types of drive shafts, the axles will be dynamically and structurally tested in order to be able to transmit power, speed and torque to the differential. The axles will be dynamically and structurally tested in order to be able to transmit power, speed and torque to the differential. Figure 3 shows the automotive driveshaft model. The cardan shaft model was designed to be as safe as possible and hence to use the most suitable shaft, with the best engine and the safest material.

Figure 3 Automotive cardan shaft model
Source: Own Elaboration (Solidworks)

Dynamic simulation

For the development of the dynamic simulation with the automotive cardan shaft (axis 1) and the motorbike cardan shaft (axis 2), the boundary conditions were established to simulate a greater precision analogous to what it would be in real life with the Blue Core engine. Angular displacements, angular velocity and angular acceleration were measured.

The gravitational constant is set to 9.81 m/s^2, the motor torque of 12.8 N-m at the output flange, at a constant speed of 4500 RPM, due to hardware limitations, the simulation time was defined from 0 to 0.50 seconds (Shigley *et al*., 2019).

For the angular displacement, the two crossheads of the automotive cardan shaft were selected, as these are the elements that generate a greater displacement in the rotation as shown in the tracings; in Figure 4 it can be seen that the crossheads have a similar displacement, indicating that there is no considerable offset that could affect the movement of the shaft.

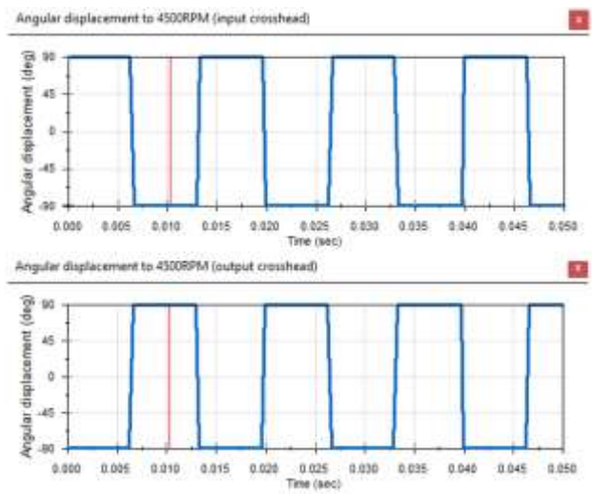

Figure 4 Angular displacement trace
Source: Own Elaboration (Solidworks)

Table 3 shows the results of the Blue Core motor with the two axes, as well as the angular velocity, maximum and minimum torque and energy consumption, which are similar to the values provided by the manufacturer.

ISSN 2523-6784

Blue Core	Axis 1	Axis 2
Angular velocity (grad/sec)	27000	27000
Minimum torque (N-m)	12.798	12.8
Maximum torque (N-m)	13.03	13.07
Minimum power consumption (Watt)	6031	6031
Maximum power consumption (Watt)	6140	6159

Table 3 Dynamic results Blue Core engine
Source: Own elaboration (Word)

Table 4 shows the dynamic results of the CBF125 TWISTER 2022 engine, obtaining results similar to those of the manufacturer.

CBF125 TWISTER 2022	Axis 1	Axis 2
Angular speed (grad/sec)	30000	30000
Minimum torque (N-m)	10.1	10.1
Maximum torque (N-m)	10.12	10.12
Minimum power consumption (Watts)	5293.5	5287
Maximum power consumption (Watt)	5293.6	5301

Table 4 CBF125 Twister 2022 engine dynamic results
Source: Own Elaboration (Word)

Structural simulation

The structural simulation by movement loads, demanded a high hardware performance, to optimise the study, a solution is to analyse a time range in the simulation, that is to say, to extend the function, this is done after obtaining the dynamic traces and identifying that the function is periodic. The selected time range is from 0.030 to 0.040 seconds, having a very small variation, the time of 0.035 seconds was selected for the demonstration of the results (Le *et al*., 2020).

Figures 5, 6 and 7 show the results of the Von Mises stress, displacement and factor of safety for the Blue Core engine with the automotive cardan shaft and Alloy Steel material.

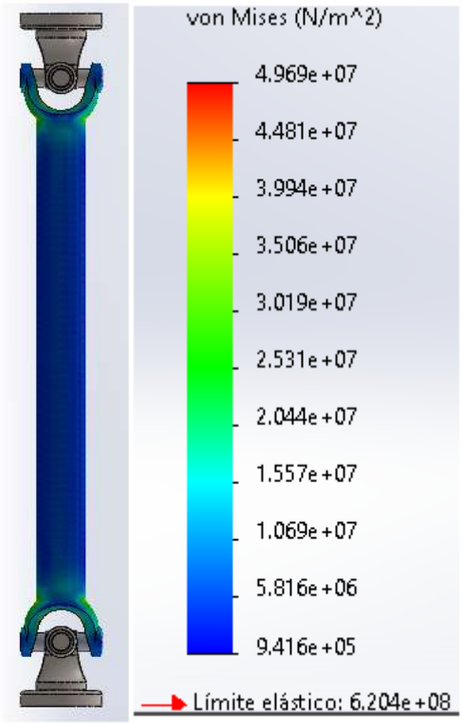

Figure 5 Von Mises stress, Blue Core engine, alloy steel
Source: Own Elaboration (Solidworks)

As shown in Figure 5, using the Blue Core motor, the maximum stress is 49.69 MPa and the minimum is 0.9416 MPa for the alloy steel automotive cardan shaft.

The maximum displacement is 7.34E-02 mm and the minimum displacement is 1.59E-04 mm, as can be seen in Figure 6.

Figure 7 shows the factor of safety, with the minimum factor of safety being 12.49, which is developed at the ends of the cardan shaft. This is reasonable, as the ends are where the power is transmitted due to the flanges and the highest stress concentrations are generated due to the change of geometry in the model.

ISSN 2523-6784

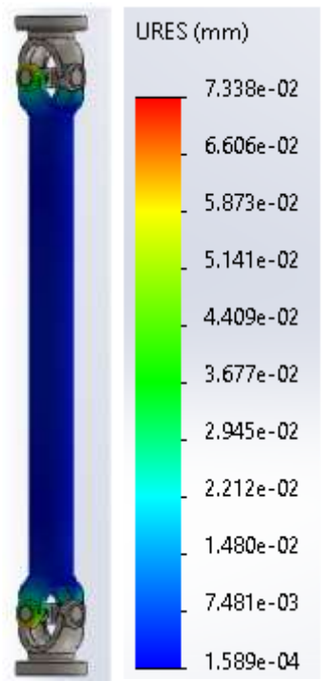

Figure 6 Displacement, Blue Core engine, alloy steel
Source: Own Elaboration (Solidworks)

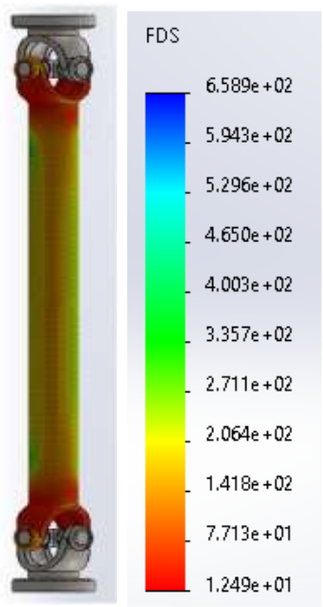

Figure 7 Factor of safety, Blue Core engine, alloy steel
Source: Own elaboration (solidworks)

Structural simulation was also carried out using moving loads to the 1045 Steel automotive cardan shaft, with the Blue Core motor at 12 N-m and 4500 RPM.

Figure 8 shows the Von Mises stresses on the 1045 steel automotive cardan shaft, the minimum stress is 0.9635 MPa and the maximum is 50.60 MPa, giving very similar stresses as with the alloy steel.

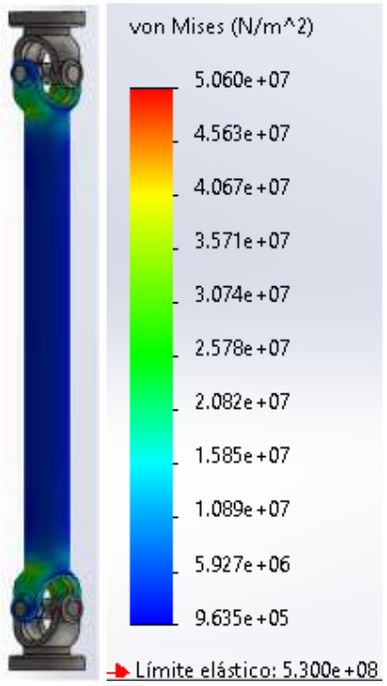

Figure 8 Von Mises stress, Blue Core engine, steel 1045
Source: own elaboration (solidworks)

The maximum displacement obtained in the 1045 steel is 7.66E-2 mm and the minimum is 1.65E-4 mm, giving larger displacements when compared to those obtained in the simulation with the alloy steel, as can be seen in Figure 9.

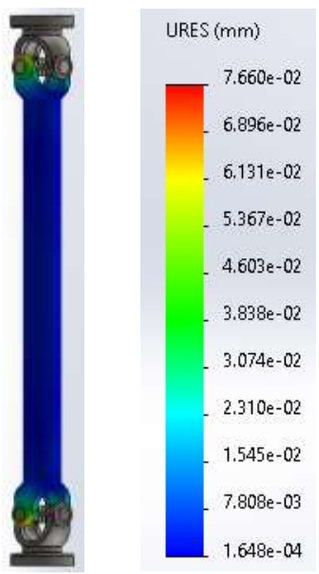

Figure 9 Displacement, Blue Core engine, steel 1045
Source: Own Elaboration (Solidworks)

Figure 10 shows the safety factor with the Blue Core motor and the automotive cardan shaft made of 1045 material, obtaining a minimum safety factor of 10.48, which is developed at the ends of the shaft.

ISSN 2523-6784

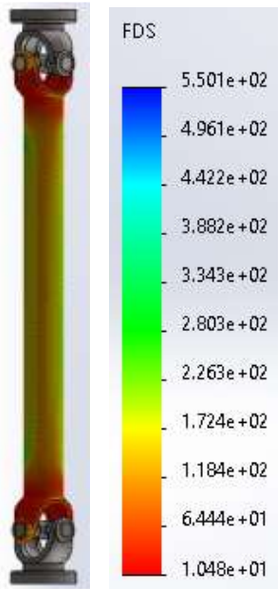

Figure 10 Safety factor, Blue Core engine, 1045 steel.
Source: Own Elaboration (Solidworks)

The same simulations were carried out for the cardan shaft of the trolley motor, using the Blue Core motor and the two types of steel, alloy and 1045; Table 5 shows the results of the structural simulations, such as: Von Mises stress, displacements and safety factor.

Blue Core Engine	Alloy steel shaft 2	AISI-1045 steel shaft 2
Von mises minimum (MPa)	0.6687	0.6685
Von mises maximum (MPa)	223.20	226.60
Minimum displacement (mm)	4.16E-05	4.72E-05
Maximum displacement (mm)	5.03E-01	5.24E-01
Minimum Factor of Safety	2.779E+00	2.339E+00
Maximum factor of safety	9.278E+02	7.928E+02

Table 5 Blue core engine structural results
Source: Own Elaboration (Word)

As can be seen in Table 5, the results for the drive shaft of the motor trolley with the Blue Core engine, the minimum Von Mises stress for the alloy steel is 0.6687 MPa, while the minimum for the 1045 steel is 0.6885 MPa, the maximum displacements for the alloy steel and 1045 are 5.03E-01 and 5.24E-01 mm, respectively. The minimum factor of safety was obtained for 1045 steel as 2.339, and for alloy steel as 2.779.

Once the simulations were carried out with the Blue Core engine, the same simulations were carried out, but now with the CBF125 TWISTER 2022 engine, at 10.11 N-m at 5000 RPM, using the two types of cardan shafts, with the two types of material, alloy steel and 1045 steel. The results of these simulations are presented in Table 6.

CBF125 TWISTER 2022	Alloy steel shaft 1	AISI-1045 steel shaft 1	Alloy steel shaft 2	AISI-1045 steel shaft 2
Von mises minimum (MPa)	0.8593	0.8748	0.8494	0.8496
Von mises maximum (MPa)	61.39	62.46	275.60	279.80
Minimum displacement (mm)	1.12E-04	9.43E-05	5.08E-05	5.71E-05
Maximum displacement (mm)	8.81E-02	9.19E-02	6.21E-01	6.47E-01
Minimum Factor of Safety	1.011E+01	8.486E+00	2.251E+00	1.894E+00
Maximum factor of safety	7.220E+02	6.059E+02	7.304E+02	6.238E+02

Table 6 Structural results CBF125 TWISTER 2022 engine
Source: Own Elaboration (Word)

The minimum Von Mises stress is 0.8494 MPa and is obtained with the trolley cardan shaft and the alloy steel. The maximum displacement was obtained with the motor trolley shaft and 1045 steel which was 6.47E-01 mm, likewise, with this shaft the minimum safety factor of 1.89 was obtained, these results are using the CBF125 Twsiter 2022 engine. For the same data, the maximum total deformation, the maximum Von Mises stress and the minimum safety factor can be seen.

In Figure 11, you can see the comparison of all the simulations for the Blue Core (simulation 1) and CBF125 Twister 2022 (simulation 2) engines with the automotive cardan shaft and the motorbike trolley cardan shaft, as well as the different types of materials used, alloy steel and 1045 steel. The maximum Von Mises stress was obtained in the simulation of the CBF125 Twister 2022 engine, with the automotive cardan shaft and AISI 1045 steel, being 279.80 MPa. With the alloy steel material, it gave a stress of 275.60 MPa, slightly less than the previous one. While the lowest Von Mises stress was for the Blue Core engine simulation, with the automotive shaft and alloy steel, resulting in 49.69 MPa. The above is shown in Figure 11.

ISSN 2523-6784

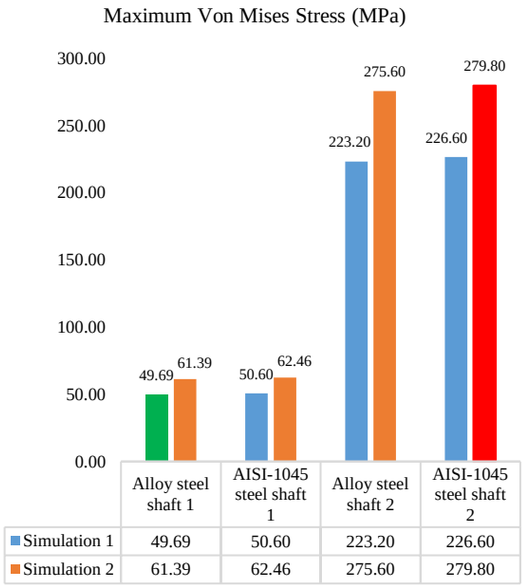

Figure 11 Von Mises stress (MPa)
Source: Own Elaboration (Excel)

Figure 12 shows the maximum displacements with the two types of motors used, the maximum deformation was 0.647 mm, with the CFB125 Twister 2022 motor, the AISI 1045 steel and the cardan shaft of the motor car. For the simulation of the Blue Core engine, alloy steel and the automotive cardan shaft, a minimum deformation of 7.34E-02 mm was obtained.

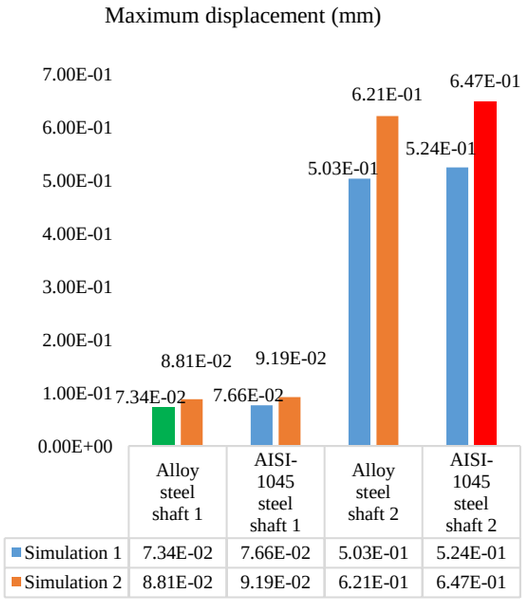

Figure 12 Dynamic displacements (mm)
Source: Own Elaboration (Excel)

The minimum safety factor was 1.894 with the CBF125 Twister 2022 engine in the automotive cardan shaft with AISI 1045 steel material. The simulation with the Blue Core engine and the automotive cardan shaft with alloy steel achieved a minimum safety factor of 1.249E+01. Both safety factors are acceptable as they are within the established range. However, the latter has a higher structural safety criterion for the boundary conditions at which both shafts were simulated, as can be seen in Figure 13.

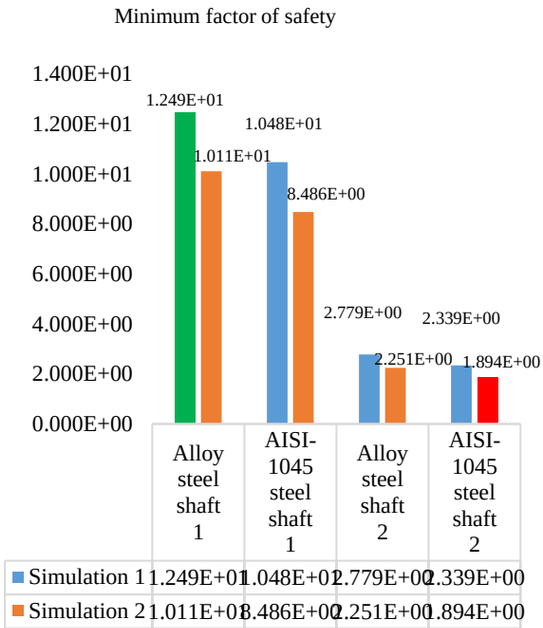

Figure 13 Safety factor
Source: Own Elaboration (Excel)

Conclusions

Based on the results obtained and having analysed each of the graphs above, by means of the structural simulation of dynamic loads, the structural element that stands out with the minimum Von Mises stress, the minimum deformation and the minimum safety factor, the automotive cardan shaft model with the alloy steel material and the simulated boundary conditions described in the specifications of the Blue Core engine (simulation 1), can be distinguished.

ISSN 2523-6784

References

Ciornei, F., Alaci, S., Romanu, I., Mihai, I., & Tibu, G. (2019). Kinematical analysis of a generalized Cardanic joint. IOP Conference Series: Materials Science And Engineering, 477, 012037. https://doi.org/10.1088/1757-899x/477/1/012037

HUERTA-GAMEZ, H., HERRERA-OLIVARES, E., ZUÑIGA-CERROBLANCO, J., & AGUILAR-MORENO, A. (2020). Análisis estructural de chasis prototipo para automóvil tipo SAE BAJA. Revista De Ingenieria Innovativa, 12-19. https://doi.org/10.35429/joie.2020.13.4.12.19

Le, V., Quang Nguyen, T., Quan Le, H., Tran, P., Nguyen, T., & Nguyen, X. (2020). Analysis of Torsional Vibration Reduction on Automobile Cardan Shaft by using Composite Materials. IOP Conference Series: Materials Science And Engineering, 886(1), 012013. https://doi.org/10.1088/1757-899x/886/1/012013

Shigley, J., Nisbett, J., & Budynas, R. (2019). Diseño en ingeniería mecánica de Shigley. McGraw-Hill Interamericana.

ISSN 2523-6784

Article **Journal of Systematic Innovation**
June 2022 Vol.6 No.18 27-32

Adjustable testbench system to stretch optical fiber

Plataforma de pruebas ajustable para estrechar fibra óptica

TALAVERA-VELÁZQUEZ Dimas†, MARTÍNEZ-TELLO Josué, GUTIÉRREZ-VILLALOBOS José Marcelino* and RIVAS-ARAIZA Edgar Alejandro

Universidad de Guanajuato Campus Celaya-Salvatierra, Av. Javier Barrios Sierra 201 Col. Ejido de Santa María del Refugio C.P. 38140 Celaya, -Gto. México
Universidad Autónoma de Querétaro, Cerro de las Campanas s/n, C.P. 76010, Querétaro, Querétaro, México

ID 1st Author: *Dimas, Talavera-Velázquez* / **ORC ID**: 0000-0002-8074-1647, **CVU CONACYT ID**: 85034

ID 1st Co-author: *Josué, Martinez-Tello* / **ORC ID**: 0000-0001-6014-4995

ID 2nd Co-author: *José Marcelino, Gutierrez-Villalobos* /**ORC ID**: 0000-0001-5947-1489, **Research ID Thomson**: S-7666-2018, **CVU CONACYT ID**: 173461

ID 3rd Co-author: *Edgar Alejandro, Rivas-Araiza* /**ORC ID**: 0000-0001-, **Research ID Thomson**: S-7666-2018, **CVU CONACYT ID**: 44036

DOI: 10.35429/JSI.2022.18.6.27.32 Received March 14, 2022; Accepted June 29, 2022

Abstract

Actually, the use of optical fiber has been extended to several applications, not only its use for telecommunications; nowadays, optical fiber is used for sensor construction and instrumentation. For that reason, modifications and deformations in optical fiber sections are required and in order to observe how light transition is performed through to the fiber. The construction of this platform has the main objective to accomplish stretching test with different tensions on the fiber, different exposition terms to the electric arc and finally the gap between electrical electrodes to modify the affectations on the fiber, that are applied on the fiber. The different parts this system is conformed with, are presented in this work and the main features of each stage.

Instrumentation, Optical fiber stretching, tensions, Tensions, deformations

Resumen

En la actualidad, el uno de fibra óptica se ha extendido a diversas aplicaciones ya no solo en el campo de las telecomunicaciones, ahora se emplea en la construcción de sensores e instrumentación, para lo cual se requiere hacer modificaciones o deformaciones en secciones de la fibra óptica y observar como se ve alterada la transmisión de luz dentro de la fibra. La construcción de esta plataforma tiene como objetivo realizar pruebas de estrechamiento con diferentes tensiones sobre la fibra, diferentes periodos de tiempo de exposición al arco eléctrico y finalmente la separación entre electrodos para modificar las afectaciones que se pueden infringir sobre la fibra. El trabajo describe las diferentes partes que conforman el sistema y las principales características de cada etapa.

Instrumentación, Estrechamiento de Fibra óptica, Tensiones, Deformaciones

Citation: TALAVERA-VELÁZQUEZ Dimas, MARTÍNEZ-TELLO Josué, GUTIÉRREZ-VILLALOBOS José Marcelino and RIVAS-ARAIZA Edgar Alejandro. Adjustable testbench system to stretch optical fiber. Journal of Systematic Innovation. 2022. 6-18: 27-32

† Researcher contributing as first author.

Introduction

Devices of stretching optical fiber filament have been used as sensors, using the optical property of the evanescent field during signal transitions. Therefore, the optical fiber interaction with several material such as alcohol, silicon oxide and even construction material, is improved and amplified by this property. In some cases alcohol for example, in medical areas for instance optical fiber is used to sense human body fluids; silicon oxide used to improve the effects of Raman spreading, also in force and temperature measurements; with construction material, the concrete deformation cab be measured by deformation of the optical fiber filament as well. This research has as mail purpose to design, build and test a stretching machine for micro-optical glass fibers employing an electric arc, with the idea of softening glass optical fibers and applying different tensions on the fiber filaments.

At the biggening of the XXI century, many investigations on stretched glass optical fiber (SGOF) took place, using the property of evanescent field for optical signals SGOF. During the last eight years, the same effect has been observed on micro and nano fibers, in this case µSGOF and nSGOF, which have shown better results, obtaining low lost by attenuation and using the no-lineal effects of the evanescent field. The sensors based on µSGOF have also shown better results on alcohols, they are manufactured by butane gas flame as mention by Shan 2013. µSGOF are also an option for remote detection such as humidity, refractive index detection, steam detection, biomedicines, chemical analysis, environmental engineering and car industry, Razak 2017. Since The µSGOF have proved to have optical power leak guided, they are used in sensors for surface plasmon resonance on glass optical fibers, as described in Jafari 2017. For some sensors, a thin metal film is applied and to polish the narrow part of the cone of the optical fiber, it needs to be submerged in hydrofluoric acid, which can lead to 40 µm diameters, as explained by Yu 2014. Many other applications are presented by the author Lim 2012 and Lee 2019, for example: no-linear optical effects amplified, including Brillouin dispersion, Raman amplification and the generation of super continuous. Also, as mentioned by Garcia-Fernandez 2011, it is the µSGOF interferometer with its construction and tests.

Then, µSGOF are used to achieve a diabatic transmission of approximately 99% for the fundamental mode, presented by Lützler2012 and Ward 2014. Researches for a µSGOF knob resonator and Mach-Zehnder interferometer to measure temperatures and refractive indices by Gomes 2017. Finally, different laser sources are employed for to stretch optical fibers, as mentioned by Sumetsky 2010 and Gai 2012.

Therefore this prototipe, as the proposed one by Figueroa 2022, can prompt to start medical applicacion. In addition to what Garcia 2022 where a surface detector usind ultraviolet light for a robot, optical fiber light may result in an alterantive such a Time-of-Flight sensor, which are designed to sense the time light takes to go and come. Similarly to the pruposed system control, Sanchez 2022, used a fast development board what ends to be good and cheap alternative.

Stretching platform

In particular, this proposed work has the target of developing a system, that allows infringing deformations on the glass optical fiber by tension or/and different exposures to electric arcs. On one hand, the fiber can suffer several levels of tension, which is produced by a fixed clamp and a mobile one, the mobile clamp is located on a platform that is motor-shaft connected with a ball screw to displace and produce tension. On the other hand, the electric arc, it is produced in different triggering pulses, it can be a time on and a time off or several times on and off in a specific term, as it can be observed in figure 1.

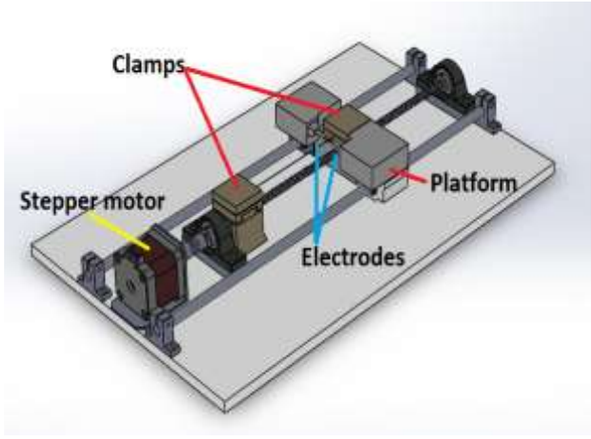

Figure 1 Basic concept of the platform

ISSN 2523-6784

Here the system has to sense the tension applied on the optical fiber, which is achieved by a strain gauge installed under the fixed clamp and its measurement is converted in newtons per meter, once the cell is characterized and linearized using measurement patterns previously. For electric arcs, there are two functions that can be modified independently, the gap between both electrodes and the triggering pulses.

Electric arc

Indeed Electric arc is generated by the flybacks converters series-connected; both consume energy from the same power source. Using a optocoupler circuit to isolate from the timer board and avoid damage to it. The circuit to generate the pulsing voltage for flyback converters is presented in figure 2a and both converters' series-connected in figure 2b, respectively.

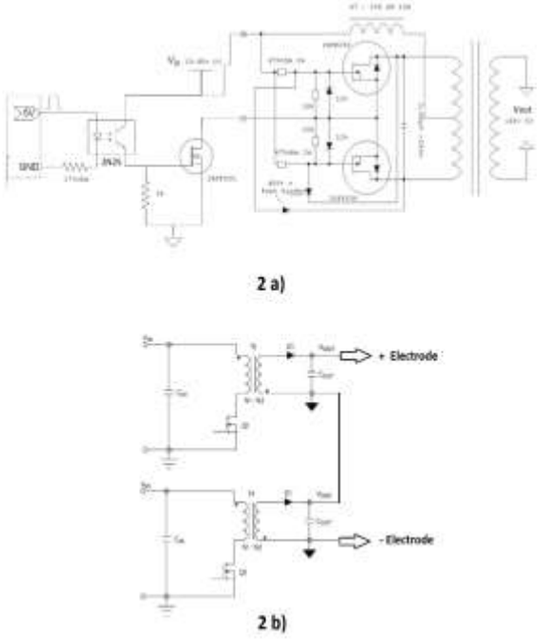

Figure 2 Schematic diagram, a) circuit to drive each fly-back converter, b) Tow converts series-connected

Then the driver circuit is supplied by 30 dc Volts, then the driver commutates at a frequency of 10 kHz, its output generates a 140 dc Volts (pulsating), after that this output is the input for each fly-back converter parallel-connected to the driver circuit; finally, the converters have an output of 10 kVdc, which generates a 20 kVdc approximately, so with this amount of voltage an electric arc is created, their terminals can be close to each other from 3 mm to 10 mm.

Movement of electrodes

Eventually, The mechanism for separating the electrodes can be observed and the rest of the system are in figure 3. They are placed on two stepper-motor mechanisms. Both motors are driven by a L293 driver circuit, that is connected and controlled by the main board (ATmega 2560).

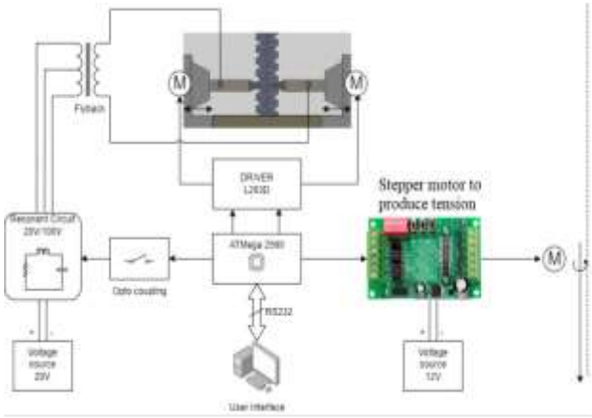

Figure 3 General block Diagram with the system stages

Tension measurement

Secondly, the stepper motor, seen in figure 1, is connected to a stepper motor Tb6560 driver as observed in figure 2. As previously mention, the tension is measured by a strain gauge connected to the ATmega board as well. Its values are sent to the microcontroller on the development board and control the tension is then applied. This connection is presented in figure 4.

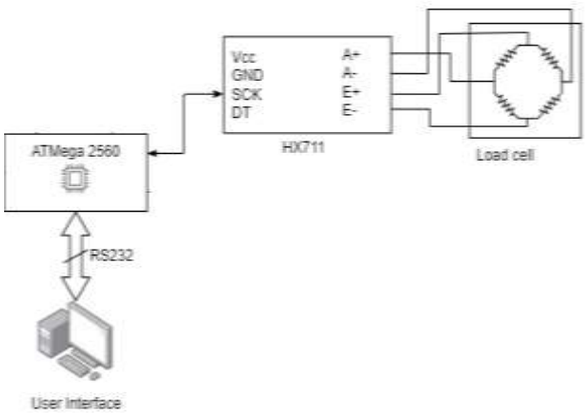

Figure 4 Strain gauge connection

Importantly, the strain gauge must be connected by means of a circuit to condition and amplify the electrical signal, so the microcontroles ADC can read that signal.

ISSN 2523-6784

System interface

Summarizing, there is a human-machine interface HMI or display, where several parameters have to be settled, for example: electrode gap, time and pulses for the electric arc. The HMI is presented in figure 5. It is communicated with the ATmega board by USB, so the complete system is controlled by the computer. Certanly, this is one of the system advantages, it can be connected to almost any Windows-compatible computer, due to the platform modularity, the system can eventually be updated to sense other variables or add more stages to the equipment. Since the system is open access user can modify it as much as necessary. It is necessaty to mention that the HMI was designed in Microsoft Visual Studio

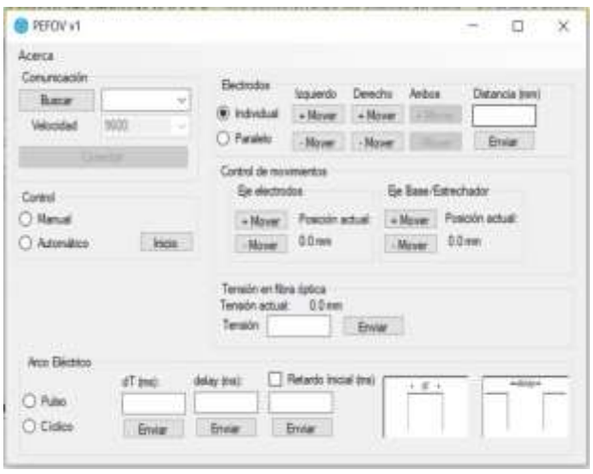

Figure 5 HMI on the computer

Equipment operation

Afterword, when the fiber is placed in position and system is connected (USB-port), application must be initialized. Then the port speed has to be settled. After that user has to set tension and time for pulses. Operation is described in figure 6. It is important to follow the sequence so the communication can be stablished.

Finally, the optical fiber filamente has to be placed in position and secured to keep in its place during tests. Later, the electrodes should be alighned so the electric arc affects the surface of the filament. The arc is strong enough to burn so its important to start with a low level arc. Furthermore, time is a key aspect, it must be short terms or pulsing discharges.

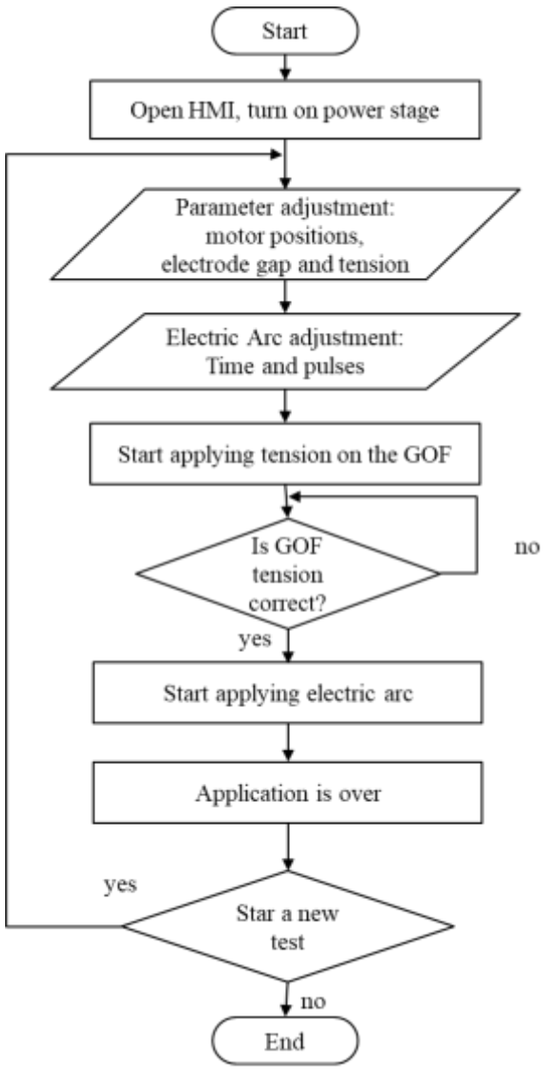

Figure 6 Stage of the stretching process

Indeed a performance of the system cab be seen on figure 7, where the fiber is settled under tention and exposed to the electric arc, in order to get stretched and therefore affectation on its structure. Also in picture 8, a close up to the electric arc exposure took places. Where the optical fiber filament is under the effects of temperature.

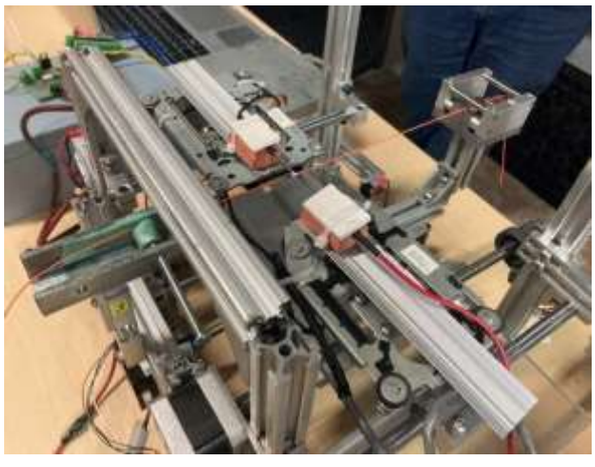

Figure 7 Stretching platform in operation

ISSN 2523-6784

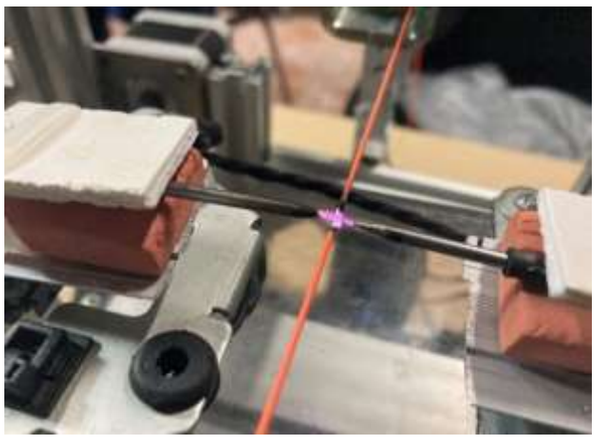

Figure 8 Close up to the electric arc

Results

Several tests took place on the system stretching, the GOF was espoused to a tension of 0.9 newtons, and the GOF had an elongation of 0.5 mm with pulsing intervals of 2 seconds on and 3 seconds off for 15 seconds, the platform has proved its effectiveness, modularity and functioning. The GOF got stretched and parameters can be adjusted as needed by user. In figure 9, the complete platform can be observed.

Figure 9 Complete stretching system

Conclusions

A robust system was built to produce electric arcs strong enough to heat up GOF at the point to stretch them. An electric circuit was developed with a software and a HMI to control periods for the electric arc and the tension applied to the optical fiber. The system is modular and open architecture to be able to incorporate more stages and add other parameters for more integrated tests. With this prototype, it is expected to start new researches on medical, construction and environmental sensors.

ISSN 2523-6784

Acknowledgments

The authors acknowledge the financial support of the University of Guanajuato to publish this work 2022 and PRODEP support 2021. Authors also recognize the facilities and the support received by Autonomous University of Queretaro to accomplish this work in 2022.
.

References

André D. Gomes and Orlando Frazao. "Microfiber Knot with Taper Interferometer for Temperature and Refractive Index Discrimination". IEEE Photonics Technology Letters, Vol. 29, No. 18, September 15, 2017. DOI: 10.1109/LPT.2017.2735185

Caibin Yu, Xiaoxiao Chen, Yuan Gong, Yu Wu, Yunjiang Rao and Gangding Peng, "Simultaneous Force and Temperature Measurement Using Optical Microfiber Asymmetrical Interferometer", Photonic Sensors, Vol. 4, No. 3, 2014, pp. 242-247. DOI:10.1007/s13320-014-0201-4

Christian Lützler, "Fabrication of Optical Microfibers". Universit at Bonn. September 2012. DOI:10.5772/31123

Donghawa Lee, Kwang Jo Lee, Jin-Hun Kim, Kyungdeuk Park, Dongjin Lee, Yoon-Ho Kim, Heedeuk Shin, "Fabrication method for ultra-long optical micro/nano-fibers", Current Applied Physics 19 (2019) 1334–1337. https://doi.org/10.1016/j.cap.2019.08.018

Figueroa Tabares, N. (2022). Plataforma de telemedicina con prototipo de dispositivo hardware para terapia respiratorias de EPOC y asma. https://repository.eia.edu.co/handle/11190/5332

García, J. D. V., Castro, J. R., & Flóres, J. E. M. (2022). "Diseño y construcción de un robot para desinfección de superficies con luz ultraviolet". Ingeniería: Ciencia, Tecnología e Innovación, 9(1), 1-15. https://doi.org/10.26495/icti.v9i1.2161

J. M. Ward, A. Maimaiti, Vu H. Le, and S. Nic Chormaic. "Optical micro-and nanofiber pulling rig". http://dr.doi.org/10.1063/1.4901098. Published online 24 November 2014.

Jalil Jafari and Rahman Nouroozi, "Fabrication and Characterization of the Fiber Optical Taper for a Surface Plasmon Resonance Sensor", International Journal of Optics and Photonics, Vol 11, No. 1, Winter-Spring, 2017. DOI:10.18869/acadpub.ijop.11.1.19

K. S. Lim, S. W. Harun, H. Arof and H Ahmad, "Fabrication and Applications of Microfiber", Selected Topics on Optical Fiber Technology", www.intechopen.com, hard cover, 668 pages, 22, February 2012. DOI: 10.5772/31123

L. Shan, G. Pauliat, G. Vienne, L. Tong y S. Lebrun, "Design of nanofibers for efficient simulated Raman scattering in the evanescent field", J. Europ. Opt. Soc. Rap. Public. 8, 13030 (2013). DOI: 10.2971/jeos.2013.13030

Liting Gai, Jin Li and Yong Zhao. "Preparation and application of microfiber resonant ring sensors: A review". Optics & Laser Technology 89 (2017) 126-136. https://doi.org/10.1016/j.optlastec.2016.10.002

M. Sumetsky, Y. Dulashko and S. Chalmi. "Fabrication of miniature optical fibre and microfiber coils". Optics and Lasers in Engineering 48 (2010) 272-275. https://doi.org/10.1016/j.optlaseng.2009.11.011

Montoya La Torre, H. N., & Jiménez Calderón, B. L. A. (2022). "Implementación de aplicaciones IoT usando el D1 mini ESP32, protocolo MQTT y servicios de IFTTT". http://repositorio.unp.edu.pe/handle/20.500.12676/3556

N. A. Razak, B. A. Hamida, N. Irawati and M. H. Habaebi, "Technique and coated with Polymer Polyaniline for Sensing Application". International Technical Postgraduate Conference. Series: Materials Science and Engineering 210 (2017). DOI:10.1088/1757-899X/210/1/012041

R. Garcia-Fernandez, A. Stiebeiner, and A. Rauschenbeutel, "Optical nanofibers and spectroscopy", Applied Physics B, May 2011. https://doi.org/10.1007/s00340-011-4730-x

Sánchez Lasheras, M. J. (2022). Implementación del control de actitud y trayectoria en un AR. Drone 2.0 mediante Simulink. http://hdl.handle.net/10251/184352

ISSN 2523-6784

Title in Times New Roman and Bold No. 14 in English and Spanish]

Surname (IN UPPERCASE), Name 1st Author†*, Surname (IN UPPERCASE), Name 1st Coauthor, Surname (IN UPPERCASE), Name 2nd Coauthor and Surname (IN UPPERCASE), Name 3rd Coauthor

Institutional Affiliation of Author including Dependency (No.10 Times New Roman and Italic)

International Identification of Science - Technology and Innovation

ID 1st Author: (ORC ID - Researcher ID Thomson, arXiv Author ID - PubMed Author ID - Open ID) and CVU 1st author: (Scholar-PNPC or SNI-CONACYT) (No.10 Times New Roman)

ID 1st Coauthor: (ORC ID - Researcher ID Thomson, arXiv Author ID - PubMed Author ID - Open ID) and CVU 1st coauthor: (Scholar or SNI) (No.10 Times New Roman)

ID 2nd Coauthor: (ORC ID - Researcher ID Thomson, arXiv Author ID - PubMed Author ID - Open ID) and CVU 2nd coauthor: (Scholar or SNI) (No.10 Times New Roman)

ID 3rd Coauthor: (ORC ID - Researcher ID Thomson, arXiv Author ID - PubMed Author ID - Open ID) and CVU 3rd coauthor: (Scholar or SNI) (No.10 Times New Roman)

(Report Submission Date: Month, Day, and Year); Accepted (Insert date of Acceptance: Use Only ECORFAN)

Abstract (In English, 150-200 words)

Objectives
Methodology
Contribution

Abstract (In Spanish, 150-200 words)

Objectives
Methodology
Contribution

Keywords (In English)

Indicate 3 keywords in Times New Roman and Bold No. 10

Keywords (In Spanish)

Indicate 3 keywords in Times New Roman and Bold No. 10

Citation: Surname (IN UPPERCASE), Name 1st Author, Surname (IN UPPERCASE), Name 1st Coauthor, Surname (IN UPPERCASE), Name 2nd Coauthor and Surname (IN UPPERCASE), Name 3rd Coauthor. Paper Title. Journal of Systematic Innovation. Year 1-1: 1-11 [Times New Roman No.10]

* Correspondence to Author (example@example.org)
† Researcher contributing as first author.

Introduction

Text in Times New Roman No.12, single space.

General explanation of the subject and explain why it is important.

What is your added value with respect to other techniques?

Clearly focus each of its features

Clearly explain the problem to be solved and the central hypothesis.

Explanation of sections Article.

Development of headings and subheadings of the article with subsequent numbers

[Title No.12 in Times New Roman, single spaced and bold]

Products in development No.12 Times New Roman, single spaced.

Including graphs, figures and tables-Editable

In the article content any graphic, table and figure should be editable formats that can change size, type and number of letter, for the purposes of edition, these must be high quality, not pixelated and should be noticeable even reducing image scale.

[Indicating the title at the bottom with No.10 and Times New Roman Bold]

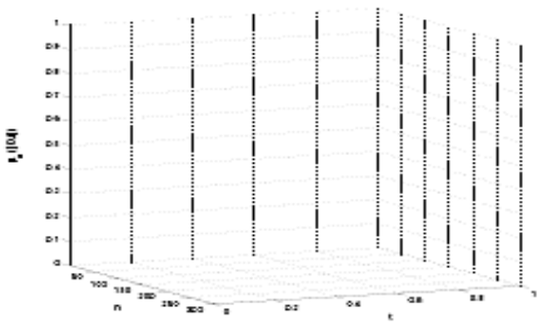

Graphic 1 Title and *Source (in italics)*

Should not be images-everything must be editable.

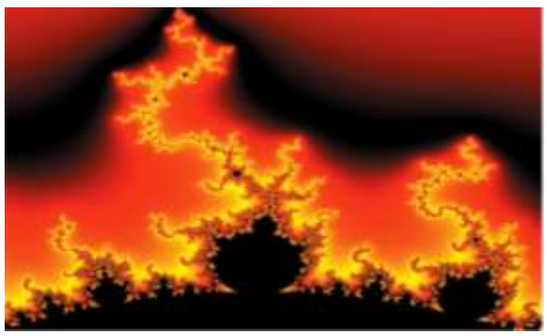

Figure 1 Title and *Source (in italics)*

Should not be images-everything must be editable.

Table 1 Title and *Source (in italics)*

Should not be images-everything must be editable.

Each article shall present separately in **3 folders**: a) Figures, b) Charts and c) Tables in .JPG format, indicating the number and sequential Bold Title.

For the use of equations, noted as follows:

$$Y_{ij} = \alpha + \sum_{h=1}^{r} \beta_h X_{hij} + u_j + e_{ij} \qquad (1)$$

Must be editable and number aligned on the right side.

Methodology

Develop give the meaning of the variables in linear writing and important is the comparison of the used criteria.

Results

The results shall be by section of the article.

Annexes

Tables and adequate sources

Thanks

Indicate if they were financed by any institution, University or company.

ISSN: 2523-6784

Conclusions

Explain clearly the results and possibilities of improvement.

References

Use APA system. Should not be numbered, nor with bullets, however if necessary numbering will be because reference or mention is made somewhere in the Article.

Use Roman Alphabet, all references you have used must be in the Roman Alphabet, even if you have quoted an Article, book in any of the official languages of the United Nations (English, French, German, Chinese, Russian, Portuguese, Italian, Spanish, Arabic), you must write the reference in Roman script and not in any of the official languages.

Technical Specifications

Each article must submit your dates into a Word document (.docx):

Journal Name
Article title
Abstract
Keywords
Article sections, for example:

1. Introduction
2. Description of the method
3. Analysis from the regression demand curve
4. Results
5. Thanks
6. Conclusions
7. References

Author Name (s)
Email Correspondence to Author
References

Intellectual Property Requirements for editing:

-Authentic Signature in Color of Originality Format Author and Coauthors

-Authentic Signature in Color of the Acceptance Format of Author and Coauthors

-Authentic Signature in Color of the Conflict of Interest Format of Author and Co-authors

ISSN: 2523-6784

Reservation to Editorial Policy

Journal of Systematic Innovation reserves the right to make editorial changes required to adapt the Articles to the Editorial Policy of the Journal. Once the Article is accepted in its final version, the Research Journal will send the author the proofs for review. ECORFAN® will only accept the correction of errata and errors or omissions arising from the editing process of the Journal, reserving in full the copyrights and content dissemination. No deletions, substitutions or additions that alter the formation of the Article will be accepted.

Code of Ethics - Good Practices and Declaration of Solution to Editorial Conflicts

Declaration of Originality and unpublished character of the Article, of Authors, on the obtaining of data and interpretation of results, Acknowledgments, Conflict of interests, Assignment of rights and Distribution

The ECORFAN-Mexico, S.C Management claims to Authors of Articles that its content must be original, unpublished and of Scientific, Technological and Innovation content to be submitted for evaluation.

The Authors signing the Article must be the same that have contributed to its conception, realization and development, as well as obtaining the data, interpreting the results, drafting and reviewing it. The Corresponding Author of the proposed Article will request the form that follows.

Article title:

- The sending of an Article to Journal of Systematic Innovation emanates the commitment of the author not to submit it simultaneously to the consideration of other series publications for it must complement the Format of Originality for its Article, unless it is rejected by the Arbitration Committee, it may be withdrawn.

- None of the data presented in this article has been plagiarized or invented. The original data are clearly distinguished from those already published. And it is known of the test in PLAGSCAN if a level of plagiarism is detected Positive will not proceed to arbitrate.

- References are cited on which the information contained in the Article is based, as well as theories and data from other previously published Articles.

- The authors sign the Format of Authorization for their Article to be disseminated by means that ECORFAN-Mexico, S.C. In its Holding Taiwan considers pertinent for disclosure and diffusion of its Article its Rights of Work.

- Consent has been obtained from those who have contributed unpublished data obtained through verbal or written communication, and such communication and Authorship are adequately identified.

- The Author and Co-Authors who sign this work have participated in its planning, design and execution, as well as in the interpretation of the results. They also critically reviewed the paper, approved its final version and agreed with its publication.

- No signature responsible for the work has been omitted and the criteria of Scientific Authorization are satisfied.

- The results of this Article have been interpreted objectively. Any results contrary to the point of view of those who sign are exposed and discussed in the Article.

Copyright and Access

The publication of this Article supposes the transfer of the copyright to ECORFAN-Mexico, SC in its Holding Taiwan for its Journal of Systematic Innovation, which reserves the right to distribute on the Web the published version of the Article and the making available of the Article in This format supposes for its Authors the fulfilment of what is established in the Law of Science and Technology of the United Mexican States, regarding the obligation to allow access to the results of Scientific Research.

Article Title:

Name and Surnames of the Contact Author and the Coauthors	Signature
1.	
2.	
3.	
4.	

Principles of Ethics and Declaration of Solution to Editorial Conflicts

Editor Responsibilities

The Publisher undertakes to guarantee the confidentiality of the evaluation process, it may not disclose to the Arbitrators the identity of the Authors, nor may it reveal the identity of the Arbitrators at any time.

The Editor assumes the responsibility to properly inform the Author of the stage of the editorial process in which the text is sent, as well as the resolutions of Double-Blind Review.

The Editor should evaluate manuscripts and their intellectual content without distinction of race, gender, sexual orientation, religious beliefs, ethnicity, nationality, or the political philosophy of the Authors.

The Editor and his editing team of ECORFAN® Holdings will not disclose any information about Articles submitted to anyone other than the corresponding Author.

The Editor should make fair and impartial decisions and ensure a fair Double-Blind Review.

Responsibilities of the Editorial Board

The description of the peer review processes is made known by the Editorial Board in order that the Authors know what the evaluation criteria are and will always be willing to justify any controversy in the evaluation process. In case of Plagiarism Detection to the Article the Committee notifies the Authors for Violation to the Right of Scientific, Technological and Innovation Authorization.

Responsibilities of the Arbitration Committee

The Arbitrators undertake to notify about any unethical conduct by the Authors and to indicate all the information that may be reason to reject the publication of the Articles. In addition, they must undertake to keep confidential information related to the Articles they evaluate.

Any manuscript received for your arbitration must be treated as confidential, should not be displayed or discussed with other experts, except with the permission of the Editor.

The Arbitrators must be conducted objectively, any personal criticism of the Author is inappropriate.

The Arbitrators must express their points of view with clarity and with valid arguments that contribute to the Scientific, Technological and Innovation of the Author.

The Arbitrators should not evaluate manuscripts in which they have conflicts of interest and have been notified to the Editor before submitting the Article for Double-Blind Review.

Responsibilities of the Authors

Authors must guarantee that their articles are the product of their original work and that the data has been obtained ethically.

Authors must ensure that they have not been previously published or that they are not considered in another serial publication.

Authors must strictly follow the rules for the publication of Defined Articles by the Editorial Board.

The authors have requested that the text in all its forms be an unethical editorial behavior and is unacceptable, consequently, any manuscript that incurs in plagiarism is eliminated and not considered for publication.

Authors should cite publications that have been influential in the nature of the Article submitted to arbitration.

Information services

Indexation - Bases and Repositories

RESEARCH GATE (Germany)
GOOGLE SCHOLAR (Citation indices-Google)
MENDELEY (Bibliographic References Manager)
REDIB (Ibero-American Network of Innovation and Scientific Knowledge- CSIC)
HISPANA (Information and Bibliographic Orientation-Spain)

Publishing Services

Citation and Index Identification H
Management of Originality Format and Authorization
Testing Article with PLAGSCAN
Article Evaluation
Certificate of Double-Blind Review
Article Edition
Web layout
Indexing and Repository
ArticleTranslation
Article Publication
Certificate of Article
Service Billing

Editorial Policy and Management

69 Street. YongHe district, ZhongXin. Taipei-Taiwan. Phones: +52 1 55 6159 2296, +52 1 55 1260 0355, +52 1 55 6034 9181; Email: contact@ecorfan.org www.ecorfan.org

Journal of Systematic Innovation

2523 6784
ISSN 2523-6784

www.ecorfan.org